6. EXPLANATORY NOTES[1]

Shipboard Scientific Party[2]

In this chapter, we have assembled information that will help the reader understand the basis for our preliminary conclusions and also help the interested investigator select samples for further analysis. This information concerns only shipboard operations and analyses described in the site reports in the *Initial Reports* volume of the Leg 134 *Proceedings of the Ocean Drilling Program*. Methods used by various investigators for shore-based analysis of Leg 134 data will be detailed in the individual scientific contributions published in the *Scientific Results* volume.

AUTHORSHIP OF SITE CHAPTERS

The separate sections of the site chapters were written by the following shipboard scientists (authors are listed in alphabetical order, no seniority is necessarily implied):

Site Summary (Collot, Greene)
Background and Objectives (Collot, Greene)
Seismic Stratigraphy (Fisher)
Operations (Foss, Stokking)
Lithostratigraphy (Goud, Quinn, Reid, Riedel, Taylor)
Biostratigraphy (Akimoto, Martinez-Rodriguez, Perembo, Riedel, Staerker)
Structural Geology (Meschede, Pelletier)
Paleomagnetism (Roperch, Stokking, Zhao)
Sediment and Fluid Geochemistry (Martin)
Igneous Petrology (Baker, Briqueu, Coltorti, Hasenaka)
Igneous Geochemistry (Baker, Briqueu, Coltorti, Hasenaka)
Physical Properties (Ask, Leonard)
Downhole Measurements (Chabernaud, Hobart, Krammer, Menger)
Summary and Conclusions (Collot, Greene)
Core Descriptions (Shipboard Scientific Party)

Following the final site chapter are summary core descriptions ("barrel sheets" and igneous rock visual core descriptions) and photographs of each core.

SURVEY AND DRILLING DATA

Geophysical survey data collected during Leg 134 fall into two categories: (1) magnetic and bathymetric data acquired during transits from Australia to Vanuatu and from Vanuatu to Fiji, and (2) data collected between sites. These data are discussed in the "Underway Geophysics" chapter (this volume), along with a brief description of all geophysical instrumentation and acquisition systems used, and a summary listing of Leg 134 navigation. The survey data used for final site selection, including both data collected during site surveys prior to Leg 134 and on short site location surveys during Leg 134, are presented in the "Seismic Stratigraphy" section of the individual site chapters in this volume. During the Leg 134 *JOIDES Resolution* surveys, single-channel seismic, 3.5- and 12-kHz echo sounder, and magnetic data were recorded across the planned drilling sites to aid site confirmation prior to dropping the beacon.

The single-channel seismic profiling system used two 80-in.[3] water guns as the energy source and a Teledyne streamer with a 100-m-long active section. These data were recorded digitally on tape using a Masscomp 561 super minicomputer, and were also displayed in real time in analog format on two Raytheon recorders using a variety of filter settings (commonly 30–140 Hz) and two different scales (commonly 1- and 2-s sweeps and 50 traces/in.).

Bathymetric data collected using the 3.5- and 12-kHz precision depth recorder (PDR) system were displayed on two Raytheon recorders. The depths were calculated on the basis of an assumed 1463 m/s sound velocity in water. The water depth (in meters) at each site was corrected for (1) the variation in sound velocity with depth using Matthews' (1939) tables, and (2) the depth of the transducer pod (6.8 m) below sea level. In addition, depths that refer to the drilling-platform level are corrected for the height of the rig floor above the water line, which gradually increased from 10.89 to 11.41 throughout the cruise (see Fig. 1).

Magnetic data were collected using a Geometrics 801 proton precession magnetometer and were then displayed on a strip chart recorder and recorded on magnetic tape for later processing.

Drilling Characteristics

Because water circulation downhole is open, cuttings are lost onto the seafloor and cannot be examined. Information concerning sedimentary stratification in uncored or unrecovered intervals may be inferred from seismic data, wireline-logging results, and from an examination of the behavior of the drill string as observed and recorded on the drilling platform. Typically, the harder a layer, the slower and more difficult it is to penetrate. A number of other factors may determine the rate of penetration, so it is not always possible to relate the drilling time directly to the hardness of the layers. Bit weight and revolutions per minute, recorded on the drilling recorder, also influence the penetration rate.

Drilling Deformation

When cores are split, many show signs of significant sediment disturbance, including the concave-downward appearance of originally horizontal bands, haphazard mixing of lumps of different lithologies (mainly at the tops of cores), and the near-fluid state of some sediments recovered from tens to hundreds of meters below the seafloor. Core deformation probably occurs during cutting, retrieval (with accompanying changes in pressure and temperature), and core handling on deck.

SHIPBOARD SCIENTIFIC PROCEDURES

Numbering of Sites, Holes, Cores, and Samples

Drilling sites are numbered consecutively from the first site drilled by the *Glomar Challenger* in 1968. A site number refers

[1] Collot, J.-Y., Greene, H. G., Stokking, L. B., et al., 1992. *Proc. ODP, Init. Repts.*, 134: College Station, TX (Ocean Drilling Program).
[2] Shipboard Scientific Party is as given in the list of participants preceding the contents.

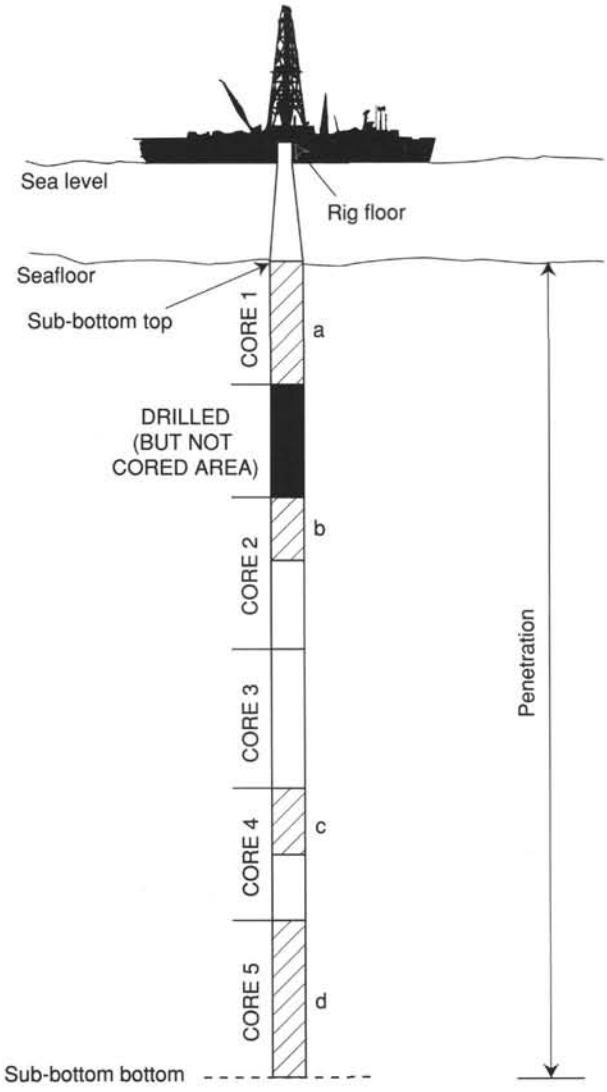

Figure 1. Diagram illustrating terms used in the discussion of coring operations and core recovery.

to one or more holes drilled while the ship was positioned over one acoustic beacon. Multiple holes may be drilled at a single site by pulling the drill pipe above the seafloor (out of the hole), moving the ship some distance from the previous hole, and then drilling another hole. In some cases, the ship may return to a previously occupied site to drill additional holes.

For all ODP drill sites, a letter suffix distinguishes each hole drilled at the same site. For example, the first hole drilled is assigned the site number modified by the suffix *A,* the second hole takes the site number and suffix *B,* and so forth. Note that this procedure differs slightly from that used by DSDP (Sites 1 through 624), but prevents ambiguity between site- and hole-number designations. It is important to distinguish among holes drilled at a site, because recovered sediments or rocks from different holes usually do not come from equivalent positions in the stratigraphic column.

The cored interval is measured in meters below seafloor (mbsf); sub-bottom depths are determined by subtracting the drill-pipe measurement (DPM) water depth (the length of pipe from the rig floor to the seafloor) from the total DPM (from the rig floor to the bottom of the hole; see Fig. 1). Note that although the echo-sounding data (from the precision depth recorders) are used to locate the site, they are not used as a basis for any further measurements.

The depth interval assigned to an individual core begins with the depth below the seafloor that the coring operation began and extends to the depth that the coring operation ended for that core (see Fig. 1). For rotary coring (RCB and XCB), each coring interval is equal to the length of the joint of drill pipe added for that interval (though a shorter core may be attempted in special instances). The drill pipe in use varies from about 9.4 to 9.8 m. The pipe is measured as it is added to the drill string and the cored interval is recorded as the length of the pipe joint to the nearest 0.1 m. For hydraulic piston coring (APC) operations, the drill string is advanced 9.5 m, the maximum length of the piston stroke.

Coring intervals may be shorter and may not necessarily be adjacent if separated by drilled intervals. In soft sediments, the drill string can be "washed ahead" with the core barrel in place, without recovering sediments. This is achieved by pumping water down the pipe at high pressure to wash the sediment out of the way of the bit and up the annulus between the drill pipe and the wall of the hole. If thin, hard, rock layers are present, it is possible to get "spotty" sampling of these resistant layers within the washed interval and thus to have a cored interval greater than 9.5 m. In drilling hard rock, a center bit may replace the core barrel if it is necessary to drill without core recovery.

Cores taken from a hole are numbered serially from the top of the hole downward. Core numbers and their associated cored intervals in meters below seafloor usually are unique in a given hole; however, this may not be true if an interval must be cored twice, because of caving of cuttings or other hole problems. Maximum full recovery for a single core is 9.5 m of rock or sediment contained in a plastic liner (6.6 cm internal diameter) plus about 0.2 m (without a plastic liner) in the core catcher (Fig. 2). The core catcher is a device at the bottom of the core barrel that prevents the core from sliding out when the barrel is being retrieved from the hole. For sediments, the core-catcher sample is extruded into a short piece of plastic liner and is treated as a separate section below the last core section. For hard rocks, material recovered in the core catcher is included at the bottom of the last section. In certain situations (e.g., when coring gas-charged sediments which expand while being brought on deck) recovery may exceed the 9.5-m maximum.

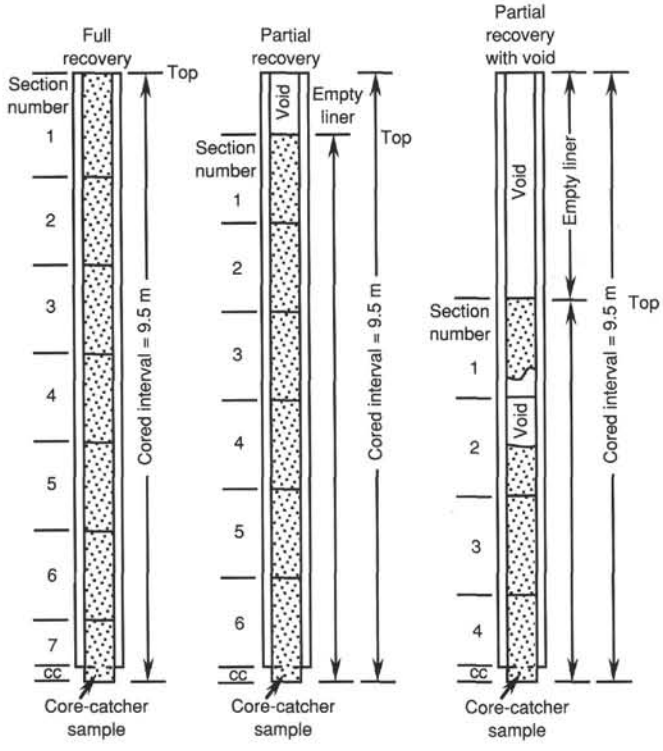

Figure 2. Diagram showing procedure used in cutting and labeling core sections.

A recovered core is divided into 1.5-m sections that are numbered serially from the top (Fig. 2). When full recovery is obtained, the sections are numbered from 1 through 7, with the last section possibly being shorter than 1.5 m (rarely, an unusually long core may require more than 7 sections). When less than full recovery is obtained, there will be as many sections as needed to accommodate the length of the core recovered; for example, 4 m of core would be divided into two 1.5-m sections and one 1-m section. If cores are fragmented (recovery less than 100%), sections are numbered serially and intervening sections are noted as void, whether shipboard scientists believe that the fragments were contiguous *in-situ* or not. In rare cases a section less than 1.5 m may be cut in order to preserve features of interest (e.g., lithological contacts).

By convention, material recovered from the core catcher is placed below the last section when the core is described, and labeled core catcher (CC); in sedimentary cores, it is treated as a separate section. The core catcher is placed at the top of the cored interval in cases where material is only recovered in the core catcher. However, information supplied by the drillers or by other sources may allow for more precise interpretation as to the correct position of core-catcher material within an incompletely recovered cored interval.

Igneous rock cores are also cut into 1.5-m sections that are numbered serially; individual pieces of rock are then each assigned a number. Fragments of a single piece are assigned a single number and individual fragments are identified alphabetically. The core-catcher sample is placed at the bottom of the last section and is treated as part of the last section rather than separately. Scientists completing visual core descriptions describe each lithologic unit, noting core and section boundaries only as physical reference points.

When, as is usually the case, the recovered core is shorter than the cored interval, the top of the core is equated with the top of the cored interval by convention in order to achieve consistency in handling analytical data derived from the cores. Samples removed from the cores are designated by distance measured in centimeters from the top of the section to the top and bottom of each sample removed from that section. In curated hard-rock sections, sturdy plastic spacers are placed between pieces that did not fit together in order to protect them from damage in transit and in storage; therefore, the centimeter interval noted for a hard-rock sample has no direct relationship to that sample's depth within the cored interval, but is only a physical reference to the location of the sample within the curated core.

A full identification number for a sample consists of the following information: leg, site, hole, core number, core type, section number, piece number (for hard rock), and interval in centimeters measured from the top of section. For example, a sample identification of "134-827A-5H-1, 10–12 cm" would be interpreted as representing a sample removed from the interval between 10 and 12 cm below the top of Section 1, Core 5 (H designates that this core was taken during hydraulic piston coring) of Hole 827A during Leg 134.

All ODP core and sample identifiers indicate core type. The following abbreviations are used: R = rotary core barrel (RCB); H = hydraulic piston core (HPC; also referred to as APC, or advanced hydraulic piston core); P = pressure core sampler; X = extended core barrel (XCB); B = drill-bit recovery; C = center-bit recovery; I = *in-situ* water sample; S = sidewall sample; W = wash-core recovery; and M = miscellaneous material. APC, XCB, RCB, and W cores were cut on Leg 134.

Core Handling

Sediments

As soon as a core is retrieved on deck, a sample is taken from the core catcher and given to the paleontological laboratory for an initial age assessment. The core is then placed on the long horizontal rack, and gas samples may be taken by piercing the core liner and withdrawing gas into a vacuum tube. Voids within the core are sought as sites for gas sampling. Some of the gas samples are stored for shore-based study, but others are analyzed immediately as part of the shipboard safety and pollution-prevention program. Next, the core is marked into section lengths, each section is labeled, and the core is cut into sections. Interstitial water (IW) and organic geochemistry (OG) samples are then taken. (The practice of taking OG samples was discontinued during Leg 134; the sections taken will be returned to the cores.) In addition, some headspace gas samples are scraped from the ends of cut sections on the catwalk and sealed in glass vials for light hydrocarbon analysis. Each section is then sealed at the top and bottom by gluing on color-coded plastic caps—blue to identify the top of a section and clear for the bottom. A yellow cap is placed on the section ends from which a whole-round sample has been removed and the sample code (e.g., IW) is written on the yellow cap. The caps are usually attached to the liner by coating the end liner and the inside rim of the cap with acetone, and then the caps are taped to the liners.

The cores then are carried into the laboratory, where the sections are again labeled using an engraver to permanently mark the full designation of the section. The length of the core in each section and the core-catcher sample are measured to the nearest centimeter; this information is logged into the shipboard CORELOG database program.

Whole-round sections from APC and XCB cores are normally run through the multisensor track (MST). The MST includes the gamma-ray attenuation porosity evaluator (GRAPE) and compressional wave (*P*-wave) logger devices,

which measure bulk density, porosity, and sonic velocity, and also includes a meter that determines the volume magnetic susceptibility. At this point, whole-round samples for physical properties (PP) and structural analysis are taken. In well-lithified sedimentary cores, the core liner is split and the top half removed so that the whole-round core can be observed before choosing the samples. Relatively soft sedimentary cores are equilibrated to room temperature (approximately 3 hr) and thermal conductivity measurements are performed on them.

Cores of soft material are split lengthwise into working and archive halves. The softer cores are split with a wire or saw, depending on the degree of induration. Harder cores are split with a band saw or diamond saw. The wire-cut cores are split from the bottom to top, so investigators should be aware that older material could have been transported up the core on the split face of each section.

The working half of the core is sampled for both shipboard and shore-based laboratory studies. Each extracted sample is logged into the sampling computer database program by the location and the name of the investigator receiving the sample. Records of all removed samples are kept by the curator at ODP. The extracted samples are sealed in plastic vials or bags and labeled. Samples are routinely taken for shipboard physical properties analysis. These samples are subsequently used for analyses of total carbonate (by coulometer) and organic carbon (by CNS elemental analyzer) and the data are reported in the site chapters.

The archive half is visually described. Smear slides are made from samples taken from the archive half and are supplemented by thin sections taken from the working half. Most archive sections are run through the cryogenic magnetometer. The archive half is then photographed with both black-and-white and color film, a whole core at a time. Close-up photographs (black and white) are taken of particular features for illustrations in the summary of each site, as requested by individual scientists.

Both halves of the core are then put into labeled plastic tubes, sealed, and transferred to cold-storage space aboard the drilling vessel. At the end of the leg, the cores are transferred from the ship in refrigerated airfreight containers to cold storage at the Gulf Coast Repository at the Ocean Drilling Program, Texas A&M University, College Station, Texas.

Igneous and Metamorphic Rocks

Igneous and metamorphic rock cores are handled differently from sedimentary cores. Once on deck, the core catcher is placed at the bottom of the core liner and total core recovery is calculated by shunting the rock pieces together and measuring to the nearest centimeter; this information is logged into the shipboard core-log database program. The core is then cut into 1.5-m-long sections and transferred into the lab.

The contents of each section are transferred into 1.5-m-long sections of split core liner, where the bottom of oriented pieces (i.e., pieces that clearly could not have rotated top to bottom about a horizontal axis in the liner) are marked with a red wax pencil. This is to ensure that orientation is not lost during the splitting and labeling process. The core is then split into archive and working halves. A plastic spacer is used to separate individual pieces and/or reconstructed groups of pieces in the core liner. These spacers may represent a substantial interval of no recovery. Each piece is numbered sequentially from the top of each section, beginning with number 1; reconstructed groups of pieces are assigned the same number, but are lettered consecutively. Pieces are labeled only on external surfaces. If the piece is oriented, an arrow is added to the label pointing to the top of the section.

The working half of the hard-rock core is then sampled for shipboard laboratory studies. Records of all samples are kept by the curator at ODP.

The archive half is visually described, then photographed with both black-and-white and color film, one core at a time. Both halves of the core are then shrink-wrapped in plastic to prevent rock pieces from vibrating out of sequence during transit, put into labeled plastic tubes, sealed, and transferred to cold-storage space aboard the drilling vessel. As with the other Leg 134 cores, they are housed in the Gulf Coast Repository.

SEDIMENT CORE DESCRIPTION FORMS

Sediment core description forms (Fig. 3), or "barrel sheets," summarize data obtained during shipboard analyses of each sediment core. The following discussion explains the ODP conventions used in compiling the core description forms and the exceptions to these procedures adopted by Leg 134 scientists. Barrel sheets for each core are included in the back of this volume.

Core Designation

Cores are designated using leg, site, hole, core number, and core type as previously discussed (see "Numbering of Sites, Holes, Cores, and Samples" section, this chapter). In addition, the cored interval is specified in terms of meters below seafloor (mbsf). On Leg 134, these depths were based on the drill-pipe measurements, as reported by the SEDCO coring technician and the ODP Operations Superintendent.

Paleontological Data

Microfossil abundance, preservation, and zone assignment, as determined by the shipboard paleontologists, appear on the core description form under the heading "Biostrat. Zone/Fossil Character." The chronostratigraphic unit, based on paleontological results, is shown in the "Time-Rock Unit" column. The zonations and terms used in reporting fossil abundance and preservation are discussed in the "Biostratigraphy" section of this chapter.

Paleomagnetic, Physical Properties, and Chemical Data

Columns are provided on the core description form to record paleomagnetic results (normal and reversed polarity intervals), physical properties values (wet-bulk density, grain density, porosity, water content, and compressional velocity), and chemical data (percentages of total carbonate determined from coulometer analyses and of organic carbon by gas chromatography). Additional information on shipboard procedures for collecting these data appears in the "Paleomagnetism," "Physical Properties," and "Inorganic Geochemistry" sections of this chapter.

Graphic Lithology Column

The lithological classification scheme of Mazzullo et al. (1987) was used in a slightly modified form on Leg 134. The classification adopted is outlined in the "Sedimentology" section of this chapter. The only significant modifications are the division of volcaniclastic sediment into two types, pyroclastic and epiclastic, and the division of fine pyroclastic sediment into "fine ash" and "coarse ash." Sediment type reflecting the classification system is graphically represented on the core description forms using the symbols illustrated in Figure 4. "Fine ash" and "coarse ash" are represented by different symbols, but no new symbol is introduced for the modification made in the epiclastic sediment classification. Instead, the symbolic designation for epiclastic sediments on

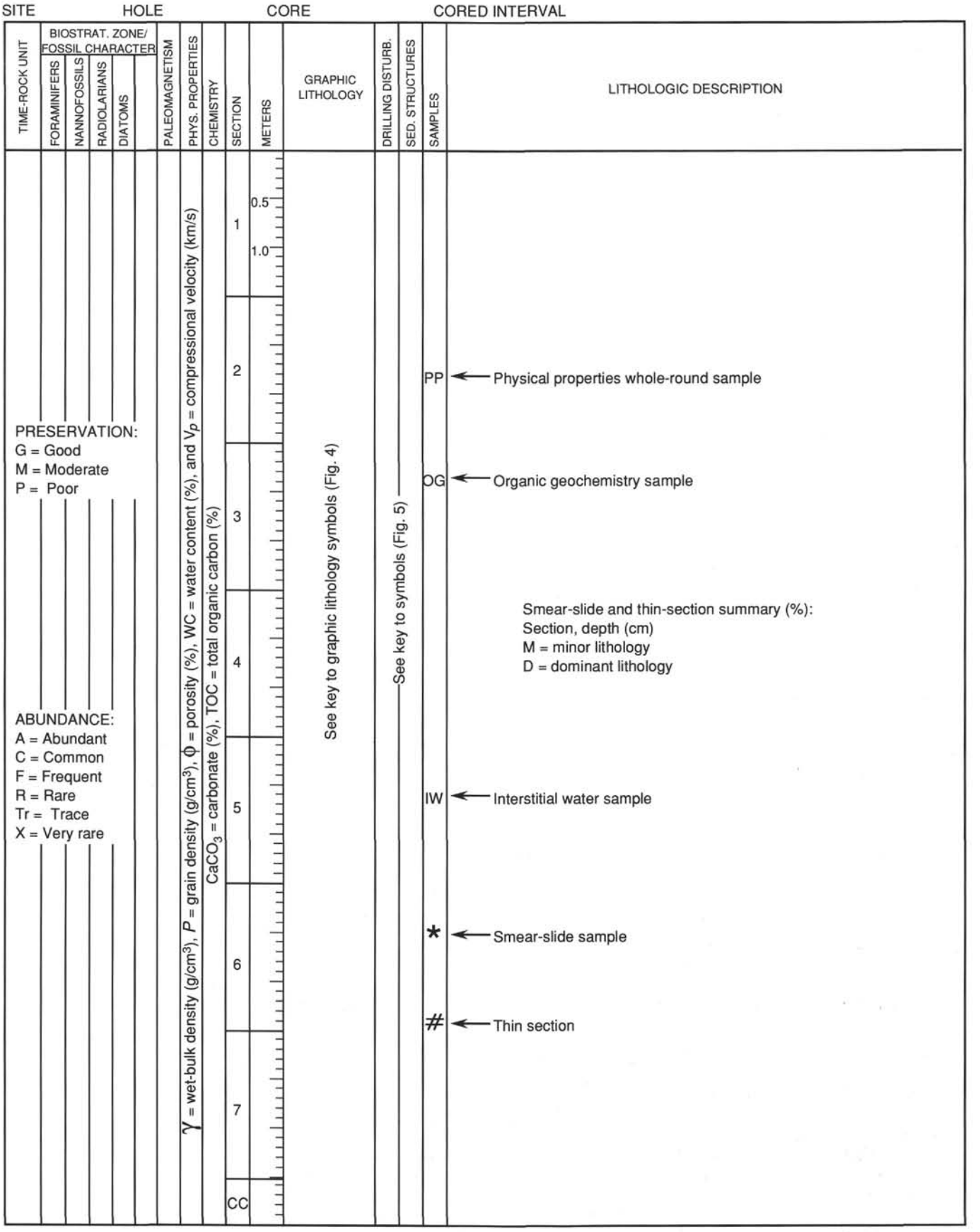

Figure 3. Core description form ("barrel sheet") used for sediments and sedimentary rocks.

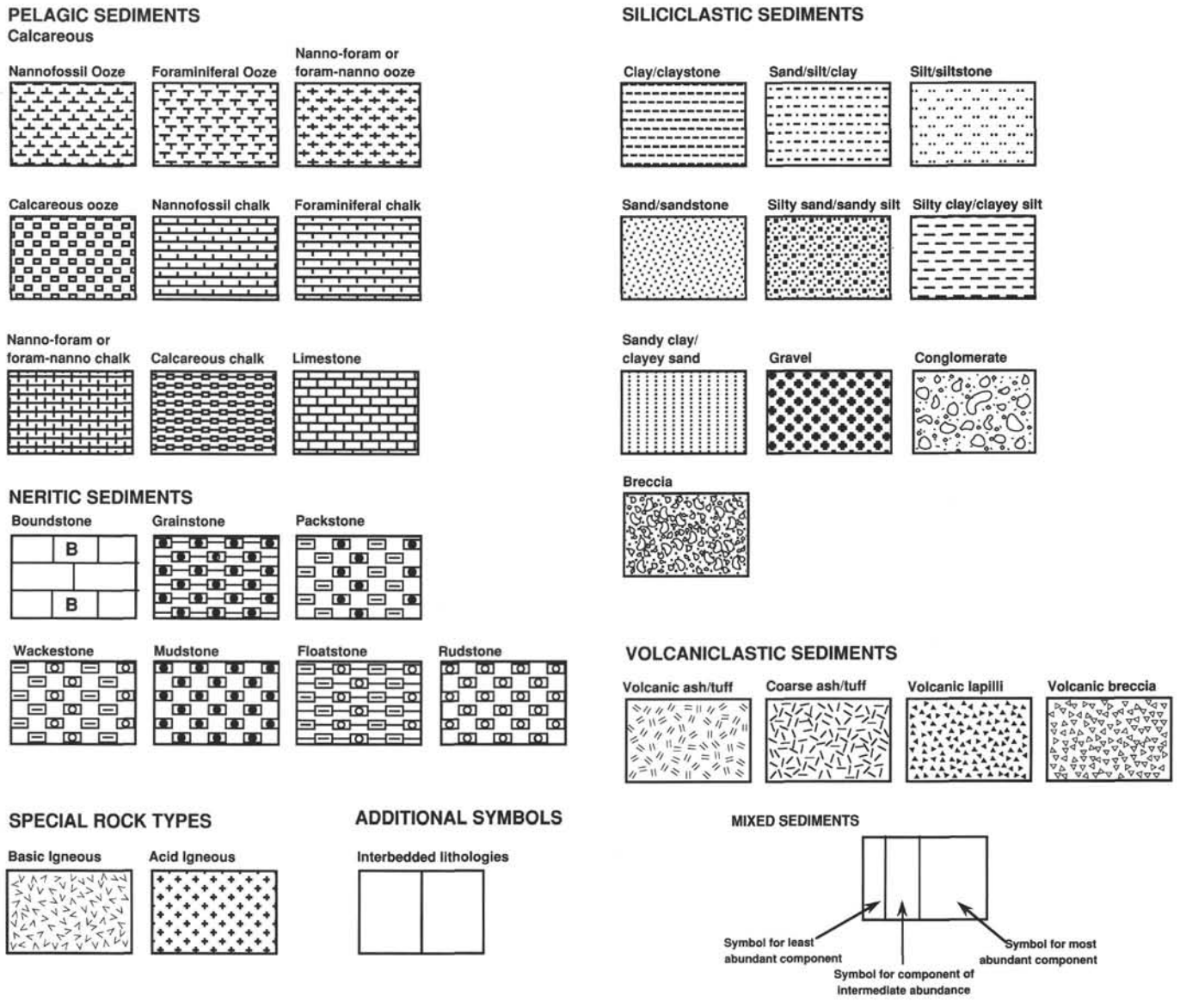

Figure 4. Key to symbols used in the graphic lithology column on the core description form shown in Figure 3, in the lithologic unit summaries in the "Lithostratigraphy" sections of site chapters, and in the master columns in the "Summary and Conclusions" sections of site chapters.

the core description form is the same as for siliciclastic rocks (sand, silt, etc.); differentiation is made in the text in the designation of "volcanic silt," "volcanic sand," etc. Intervals of igneous rocks intercalated with sedimentary material described by igneous petrologists are indicated by the symbol "IM" in the graphic lithology column (see the "Hard-Rock Core Description Forms" section in this chapter).

Sediment Disturbance

The coring techniques used may result in varying degrees of disturbance of the recovered core material. Observations of drilling-related disturbance are recorded in the "Drilling Disturbance" column on the core description form using symbols in Figure 5.

The following disturbance categories are recognized for unlithified and partially lithified sediments:

1. Slightly deformed: bedding contacts are slightly bent.
2. Moderately deformed: bedding contacts have undergone extreme bowing.
3. Highly deformed: bedding is completely disturbed, sometimes showing symmetrical diapir-like structures ("flow-in").
4. Soupy: intervals are water-saturated and have lost all aspects of original bedding.

The following categories are used to describe the degree of fracturing in lithified sediments and igneous rocks:

1. Slightly fractured: core pieces are in place and have very little drilling slurry or breccia.
2. Moderately fragmented: core pieces are in place or partly displaced, but original orientation is preserved or recognizable. Drilling slurry may surround fragments.
3. Highly fragmented: pieces are from the interval cored and probably in correct stratigraphic sequence (although they may not represent the entire section), but original orientation is totally lost.
4. Drilling breccia: core pieces have completely lost their original orientation and stratigraphic position and may be completely mixed with drilling slurry.

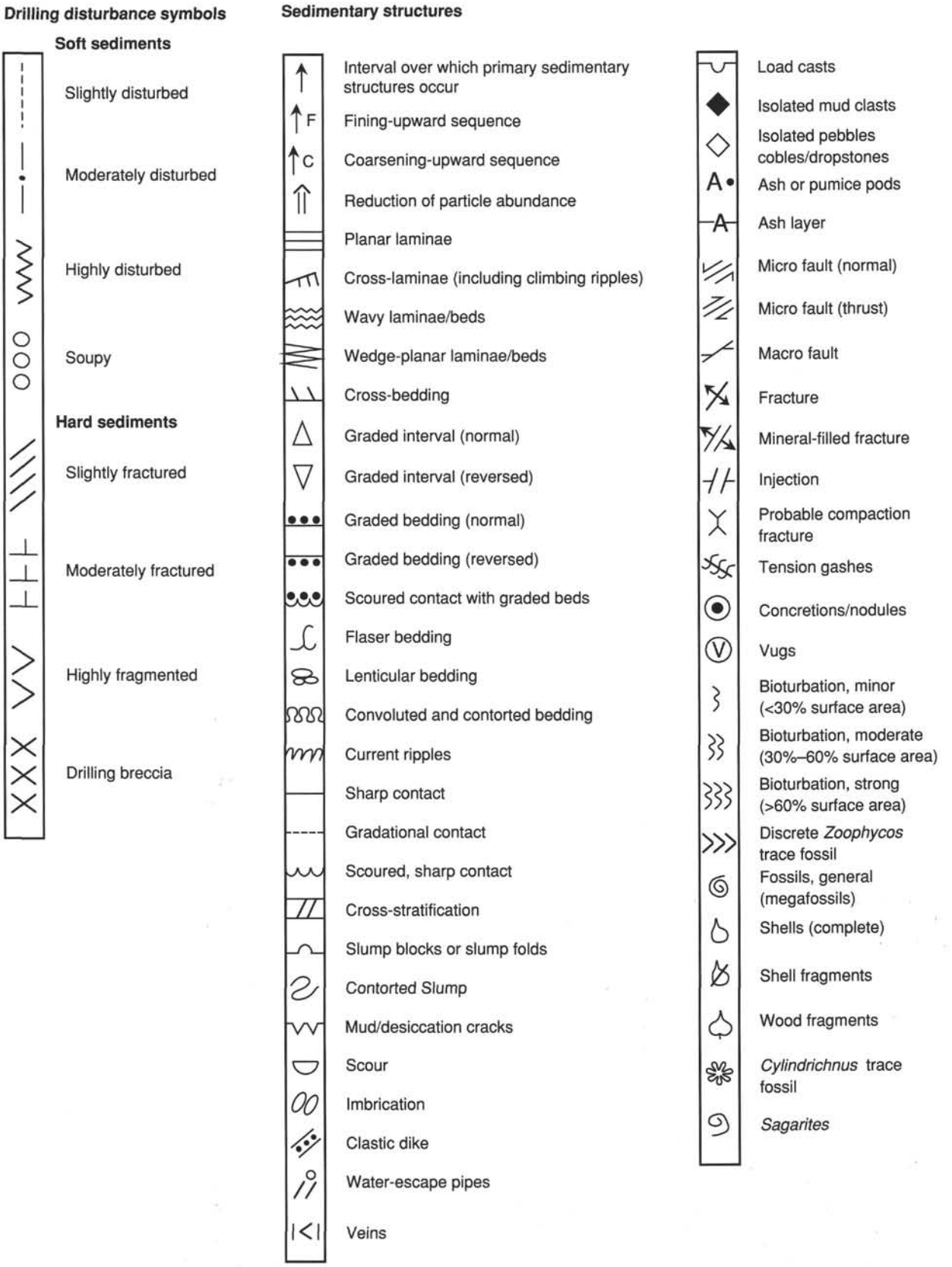

Figure 5. Symbols used for drilling disturbance and sedimentary structures on core description form shown in Figure 3.

Sedimentary Structures

Observed sedimentary structures, including fining-upward and coarsening-upward sequences are indicated in the "Sedimentary Structure" column of the core description forms. A key to symbols used on Leg 134 is given in Figure 5. Original sedimentary structures may have been destroyed in cores that have been severely disturbed by drilling.

Samples

The position of samples taken from each core for analysis is indicated by symbols in the "Samples" column in the core description form, as follows:

"★" = smear-slide samples;
"#" = location of thin sections, except igneous rock clasts;
"TS" = thin sections of igneous rock clasts;
"IW" = whole-round interstitial water geochemistry samples;
"OG" = frozen whole-round samples for organic geochemistry. (This process was discontinued during Leg 134, as directed by ODP, after some OG samples had been removed from the cores. They did not appear in photos, but will be replaced in the cores.)
"PP" = whole-round physical properties samples;
"LEO" = whole-round personal samples (taken by J. N. Leonard).

Sample position for routine physical properties measurements is indicated by a circled dot in the "Physical Properties" column, accompanied by one or more of the following symbols:

ρ = wet-bulk density (g/cm^3);
grn = grain density (g/cm^3);
ϕ = porosity (%);
w% = water content (%);
V_p = *P*-wave velocity (km/s);
V_s = shear (*S*-wave) velocity.

Sample position for routine geochemical analyses of total carbonate is indicated in the "Chemistry" column by a dot. The value on the left side of the column indicates percentage of carbonate, and the value on the right side of the column indicates total organic carbon (TOC).

Shipboard paleontologists generally base their age determinations on core-catcher samples, although additional samples from other parts of the core may be examined when required. The sample locations are shown in the appropriate column by letter codes indicating the abundance and preservation of the fossils.

Lithologic Description

The lithologic description that appears on each core description form consists of a brief summary of the major and minor lithologies observed in the core. Sedimentary structures, color, and composition of each lithology are described and, where appropriate, their distribution in the core is indicated.

Sediment color was were determined by comparison with the Geological Society of America Rock Color Chart (Munsell Soil Color Chart, 1975) immediately after the cores were split and while they were still wet, to minimize alteration due to exposure to air.

The thickness of sedimentary beds and laminae is described using the terminology of McKee and Weir (1953): very thick bedded (>100 cm thick), thick bedded (30–100 cm thick), medium bedded (10–30 cm thick), thin bedded (3–10 cm thick), and very thin bedded (1–3 cm thick). In cases where there are thin or very thin beds of a minor lithology, a description including occurrence information is included in the text, but the beds may be too thin (<10 cm) to appear in the graphic lithology column.

Smear-Slide and Thin-Section Summary

A table summarizing smear-slide descriptions appears on each core description form. The section and interval from which the sample was taken are noted, as well as identification as a *dominant* (D) or *minor* (M) lithology in the core. Grain-size distributions and biologic and lithologic components are indicated. Trace amounts of components are indicated by "Tr."

SEDIMENTOLOGY

Classification of Sediments and Sedimentary Rocks

Leg 134 used a slightly modified version of the sediment classification scheme of the Ocean Drilling Program (ODP; Mazzullo et al., 1987), which defines granular and chemical sediment types. Granular sediment consists of discrete organic (e.g., foraminifer tests, mollusc shells) or inorganic (e.g., quartz grains, rock fragments, volcanic ash) grains. Some examples of granular sediment are foraminiferal chalk, quartz sandstone, vitric ash, and bioclastic grainstone. Chemical sediment consists of minerals formed by inorganic processes, such as precipitation from solution or colloidal suspension, deposition of insoluble precipitates, or recrystallization of detrital grains. Some examples of chemical sediment are coal, halite, pyrite, and gypsum.

The ODP sediment classification scheme (Mazzullo et al., 1987) is reproduced in part below, with a single major modification for Leg 134. We subdivide volcaniclastic sediment into pyroclastic and epiclastic classes. We further subdivide fine-grained pyroclastic sediments into two size classes: material 1/16 to 2 mm in grain size (equivalent to sand in siliciclastic sediments) is described as "coarse ash" and material less then 1/16 mm (silt- and clay-size) is termed "fine ash." "Coarse tuff" and "fine tuff" are used for lithified equivalents of these size ranges. Epiclastic sediments are designated by grain size (gravel, conglomerate, sand, silt) with the modifier "volcanic" before the principal name. The only exception to this designation is epiclastic breccia, in which case "ig-lithic" or "sed-lithic" breccia is used because volcanic breccia is designated as a pyroclastic rock in the ODP classification scheme.

Granular Sediments

Classes of Granular Sediments

Variations in the relative proportions of grain types define five major classes of granular sediments: pelagic, neritic, siliciclastic, volcaniclastic, and mixed (Fig. 6). Pelagic grains are the skeletal remains of open-marine siliceous and calcareous microfauna and microflora (e.g., radiolarians, planktonic foraminifers, nannofossils) and associated organisms. Neritic grains include calcareous grains and skeletal remains (e.g., bioclasts, shallow-water benthic foraminifers, peloids) of non-pelagic origin. Siliciclastic grains are mineral and rock fragments derived from plutonic, sedimentary, and metamorphic rocks. Volcaniclastic grains include those of pyroclastic (direct products of magma degassing) and epiclastic (detritus derived from erosion of volcanic rocks) origin.

Pelagic sediments are composed of >60% pelagic and neritic grains, with a higher proportion of pelagic than neritic grains. Neritic sediments are composed of >60% pelagic and

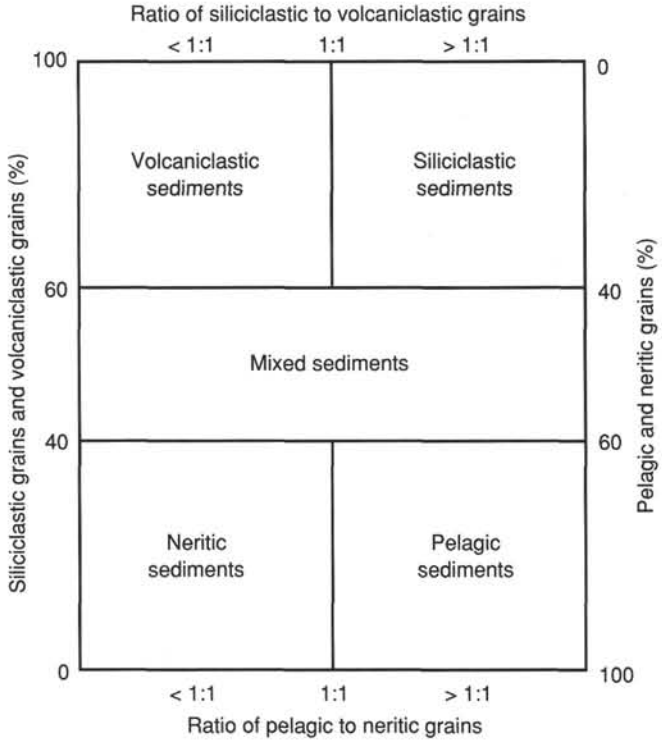

Figure 6. Diagram of granular-sediment classification scheme (modified from Mazzullo et al., 1987).

neritic grains with a higher proportion of neritic than pelagic grains. Siliciclastic sediments are composed of >60% siliciclastic and volcaniclastic grains with a higher proportion of siliciclastic than volcaniclastic grains. Volcaniclastic sediments are composed of >60% siliciclastic and volcaniclastic grains with a higher proportion of volcaniclastic than siliciclastic grains. Mixed sediments are composed of 40% to 60% siliciclastic and volcaniclastic grains, and 40% to 60% pelagic and neritic grains.

Classification of Granular Sediment

A granular sediment is classified by designating a principal name and major and minor modifiers. The principal name of a granular sediment defines its granular-sediment class; major and minor modifiers describe the texture, composition, fabric, and/or roundness of the grains themselves (Table 1).

I. Principal Names

Each granular-sediment class has a unique set of principal names, which are outlined below.

For pelagic sediment, the principal name describes composition and degree of consolidation using the following terms:

1. *Ooze:* unlithified calcareous and/or siliceous pelagic sediments;
2. *Chalk:* partially lithified pelagic sediment predominantly composed of calcareous pelagic grains;
3. *Limestone:* lithified pelagic sediment predominantly composed of calcareous pelagic grains;
4. *Radiolarite, diatomite, and spiculite:* partially lithified pelagic sediment predominantly composed of siliceous radiolarians, diatoms, and sponge spicules, respectively;
5. *Chert:* lithified pelagic sediment predominantly composed of siliceous pelagic grains.

For neritic sediment, the principal name describes texture and fabric using the following terms (after Dunham, 1962; Embry and Klovan, 1971). Note that the suffix "*-stone*" does not signify lithification.

1. *Boundstone:* components organically bound during deposition;
2. *Grainstone:* grain-supported fabric, no mud, grains <2 mm in size;
3. *Packstone:* grain-supported fabric, with intergranular mud, grains <2 mm in size;
4. *Wackestone:* mud-supported fabric, with >10% grains, grains <2 mm in size;
5. *Mudstone:* mud-supported fabric, with <10% grains;
6. *Floatstone:* matrix-supported fabric, grains >2 mm in size;
7. *Rudstone:* grain-supported fabric, grains >2 mm in size.

For siliciclastic sediment, the principal name describes texture and is assigned according to the following guidelines:

1. The Udden-Wentworth grain-size scale (Wentworth, 1922; Table 2) defines grain-size ranges and names of the textural groups (gravel, sand, silt) and subgroups (fine sand, coarse silt, etc.) that are used as the principal names of siliciclastic sediment.
2. Principal names are listed in order of increasing abundance when two or more textural groups or subgroups are present in a siliciclastic sediment (Shepard, 1954; Fig. 7).
3. The suffix *-stone* is affixed to the principal names *sand, silt,* and *clay* when the sediment is lithified.
4. Conglomerate and breccia are used as principal names of gravels with well-rounded and angular clasts, respectively. Degree of lithification is designated by a modifier before the principal name.

Volcaniclastic sediments are subdivided into two groups, pyroclastic (direct products of magma degassing) and epiclastic (detritus derived from erosion of volcanic rocks), with the principal name in each group describing texture. Pyroclastic sediment groups (Fisher and Schmincke, 1984) are defined as follows:

1. *Volcanic breccia:* pyroclasts >64 mm in diameter.
2. *Volcanic lapilli:* pyroclasts between 2 and 64 mm in diameter; when lithified, lapillistone is used.
3. *Volcanic ash:* pyroclasts <2 mm in diameter; when lithified, tuff is used. For Leg 134, this group was subdivided into two grain-size classes: coarse ash/tuff, with grains between 1/16 and 2 mm in size, and fine ash/tuff, with grains <1/16 mm in size.

Epiclastic sediments, like siliciclastic sediments, are classified based on grain texture according to the Udden-Wentworth grain-size scale. The textural principal name is preceded by the modifier "volcanic" (e.g., volcanic conglomerate, volcanic sand, volcanic silt). To avoid confusion with coarse-grained pyroclastic rock, the term "ig-lithic breccia" or "sed-lithic breccia" is used for sediment containing large angular clasts of eroded or volcanic clastic rocks, respectively. Other rules apply as listed above for siliciclastic sediments.

For mixed sediments, the principal name describes the degree of lithification, using the terms mixed sediments or sedimentary rocks.

II. Major and Minor Modifiers

The principal name of a granular-sediment class is preceded by major modifiers and followed by minor modifiers (preceded by "with") that describe the lithology of the granular sediment in greater detail (Table 1). They are most commonly used to describe composition and textures of grain

Table 1. Outline of granular-sediment classification scheme (modified from Mazzullo et al., 1987).

Sediment class	Major modifiers	Principal name	Minor modifiers
Pelagic sediment	1. Composition of pelagic and neritic grains present in major amounts 2. Texture of clastic grains present in major amounts	1. Ooze 2. Chalk 3. Limestone 4. Radiolarite 5. Diatomite 6. Spiculite 7. Chert	1. Composition of pelagic and neritic grains present in minor amounts 2. Texture of clastic grains present in minor amounts
Neritic sediment	1. Composition of neritic and pelagic grains present in major amounts 2. Texture of clastic grains present in major amounts 3. Degree of lithification	1. Boundstone 2. Grainstone 3. Packstone 4. Wackestone 5. Mudstone 6. Floatstone 7. Rudstone	1. Composition of neritic and pelagic grains present in minor amounts 2. Texture of clastic grains present in minor amounts
Siliciclastic sediment	1. Composition of all grains present in major amounts 2. Grain fabric (gravels only) 3. Grain shape (optional) 4. Sediment color (optional) 5. Degree of lithification (optional)	1. Gravel, breccia, conglomerate 2. Sand 3. Silt 4. Clay	1. Composition of all grains present in minor amounts 2. Texture and composition of siliciclastic grains present as matrix (for coarse-grained clastic sediments)
Volcaniclastic sediment	1. Composition of all grains present in major amounts 2. Texture of clastic grains present in major amounts 3. Degree of lithification (optional)	Pyroclastic: 1. Volcanic breccia 2. Lapilli 3. Coarse ash/tuff 4. Fine ash/tuff Epiclastic: 1. Volcanic conglomerate 2. Ig-lithic breccia 3. Volcanic sand 4. Volcanic silt	1. Composition of all volcaniclasts present in minor amounts 2. Composition of all neritic and pelagic grains present in minor amounts 3. Texture of clastic grains present in minor amounts
Mixed sediments	1. Composition of neritic and pelagic grains present in major amounts 2. Texture of clastic grains present in major amounts	1. Mixed sediments/ mixed sedimentary rock	1. Composition of neritic and pelagic grains present in minor amounts 2. Texture of clastic grains present in minor amounts

types present in major (>25%) and minor (10%–25%) proportions. In addition, major modifiers can be used to describe degree of lithification, grain fabric, grain shape, and sediment color. The nomenclature for major and minor modifiers is outlined below.

Composition of pelagic grains can be described with the major and minor modifiers *diatom(-aceous), radiolarian, spicule(-ar), siliceous, nannofossil, foraminifer(-al),* and *calcareous.* The terms *siliceous* and *calcareous* are generally used to describe sediments composed of siliceous or calcareous pelagic grains of uncertain origins.

Composition of neritic grains can be described with the following major and minor modifiers:

1. *Ooid* (or *oolite*): spherical or elliptical nonskeletal particles smaller than 2 mm in diameter, having a central nucleus surrounded by a rim with concentric or radial fabric.
2. *Bioclast* (or *bioclastic*): fragment of skeletal remains. Specific names such as molluscan or algal can also be used.
3. *Pellet* (or *pelletal*): a grain composed of micrite, generally lacking significant internal structure and often ovoid in shape, usually of fecal origin.
4. *Intraclast:* reworked carbonate-rock fragment or rip-up clast.
5. *Pisolite:* spherical or ellipsoidal nonskeletal particle, commonly >2 mm in diameter, with or without a central nucleus but displaying multiple concentric layers of carbonate.
6. *Peloid* (or *peloidal*): micritized carbonate particle of unknown origin.
7. *Calcareous, dolomitic, aragonitic, sideritic:* these modifiers should be used to describe the mineralogic composition of neritic grains.

Texture of siliciclastic grains is described by the modifiers *gravel(-ly), sand(-y), silt(-y),* and *clay(-ey).* Composition of siliciclastic grains can be described in terms of mineralogy and provenance using the following modifiers:

1. Mineralogy: using modifiers such as *quartz, zeolitic, lithic* (for rock fragments), or *calcareous* (for detrital clasts of calcium carbonate).
2. Provenance, or source of rock fragments (particularly in gravels, conglomerates, and breccias): using modifiers such as *volcanic, sed-lithic* (contains clasts or grains of clastic rock),

Table 2. Udden-Wentworth grain-size scale for siliciclastic sediments (Wentworth, 1922).

Millimeters	Micrometers	Phi (ϕ)	Wentworth size class	
		−20		
4096		−12	Boulder (−8 to −12 ϕ)	
1024		−10		
256		−8	Cobble (−6 to −8 ϕ)	
84		−6		Gravel
16		−4	Pebble (−2 to −6 ϕ)	
4		−2		
3.36		−1.75		
2.83		−1.5	Granule	
2.36		−1.25		
2.00		−1.0		
1.58		−0.75		
1.41		−0.5	Very coarse sand	
1.19		−0.25		
1.00		0.0		
0.84		0.25		
0.71		0.5	Coarse sand	
0.59		0.75		
1/2 — 0.50	500	1.0		
0.42	420	1.25		
0.35	350	1.5	Medium sand	Sand
0.30	300	1.75		
1/4 — 0.25	250	2.0		
0.210	210	2.25		
0.177	177	2.5	Fine sand	
0.149	149	2.75		
1/8 — 0.125	125	3.0		
0.106	106	3.25		
0.068	88	3.5	Very fine sand	
0.074	74	3.75		
1/16 — 0.0625	63	4.0		
0.063	83	4.25		
0.044	44	4.5	Coarse silt	
0.037	37	4.75		
1/32 — 0.031	31	5.0		
1.64 0.0156	15.6	6.0	Medium silt	
1/128 0.0078	7.8	7.0	Fine silt	
1/256 — 0.0039	3.9	8.0	Very fine silt	Mud
0.0020	2.0	9.0		
0.00096	0.96	10.0	Clay	
0.00049	0.49	11.0		
0.00024	0.24	12.0		
0.00012	0.12	13.0		
0.00006	0.06	14.0		

calcareous sed-lithic (contains clasts or grains of calcareous rock), *basaltic,* etc.

Volcaniclastic grain composition is described by the modifiers *ig-lithic* (rock fragments), *vitric* (glass and pumice), *volcanic sed-lithic* (contains clasts or grains of volcaniclastic rock), and *crystal* (mineral crystals), or by modifiers describing the composition of lithic grains and crystals (e.g., *feldspar* or *basaltic*).

Sediment fabric can be described by the major modifiers *grain-supported, matrix-supported,* and *imbricated.* Generally, fabric descriptors are applied only to gravels, conglomerates, and breccias.

Degree of consolidation is described using the following major modifiers: "*unlithified*" designates soft sediment that is readily deformable under the pressure of a finger, "*partially lithified*" designates firm sediment that is incompletely lithified, and "*lithified*" designates hard, cemented sediment that must be cut with a saw.

Grain shapes are described by the major modifiers *rounded, subrounded, subangular,* and *angular.* Sediment color is determined with the Munsell Chart, a standard color-comparator, and can be employed as a major modifier.

Mixed sediments are described using major and minor modifiers indicating composition and texture.

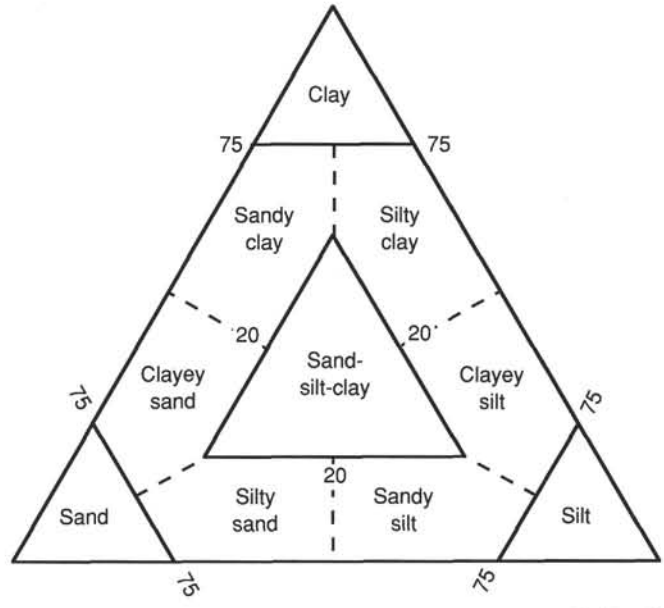

Figure 7. Ternary diagram showing principal names for siliciclastic sediments (from Shepard, 1954).

X-ray Diffraction (XRD) Analysis

A Philips ADP 3520 X-ray diffractometer was used for the X-ray diffraction (XRD) analysis of bulk samples. CuKα radiation with a Ni filter was used with a tube voltage 40 kV and a tube current 35 mA. Bulk samples were ground using the Spex 8000 Mixer Mill or with an agate mortar and pestle, and pressed into a sample holder. Samples were scanned from 2° to 70° (2Θ) in 0.02° by 1–5 steps.

BIOSTRATIGRAPHY

Chronological Framework

Four microfossil groups were examined for biostratigraphic purposes on Leg 134: calcareous nannofossils, planktonic foraminifers, benthic foraminifers, and radiolarians. Age assignments are made on the basis of core-catcher samples; however, additional samples were studied when a core-catcher sample was found to be inconclusive or otherwise unrepresentative of the core in its entirety.

The general correlation between the biostratigraphic zones and the magnetic polarity reversal record is based on the scheme of Berggren et al. (1985a, 1985c). Sample positions and the abundance, preservation, and age or zone for each fossil group are recorded on barrel sheets for each core.

Calcareous Nannofossils

Sediments recovered from Leg 134 are all of Cenozoic age. The calcareous nannofossil zonations used in this study include the schemes of Okada and Bukry (1980) and Martini (1971).

Smear slides were prepared for each sample using Norland Optical Adhesive #61 as a mounting medium. The calcareous nannofossils were examined in smear slides by standard light microscopy techniques (plane-polarized light, phase-contrast, and cross-polarized light) at a magnification of approximately 1000×.

Calcareous nannofossils often show signs of both significant etching and overgrowth; more dissolution-resistant forms add secondary calcite provided by dissolution-prone morphotypes. The following descriptive categories have been created to record the various states of preservation observed:

G = good (little or no evidence of dissolution and/or secondary overgrowth of calcite, diagnostic characteristics fully preserved);
M = moderate (dissolution and/or secondary overgrowth partially alter primary morphological characteristics, but nearly all specimens can be identified at the species level);
P = poor (severe dissolution, fragmentation, and/or secondary overgrowth with primary features largely destroyed; many specimens cannot be identified at the species and/or generic level).

Abundance estimates of the nannofossils in the smear slides were made on optimum density areas of the slide, that is, areas where most of the field was covered with sample material without appreciable piling of specimens or other material. Smear slides were examined at a magnification of 1000× and the relative abundances of individual nannofossil species in a given sample were estimated using the method proposed by Hay (1970). Six levels of abundance are recorded as follows:

H = highly abundant (101–1000 specimens per field of view);
V = very abundant (11–100 specimens per field of view);
A = abundant (1–10 specimens per field of view);
C = common (1 specimen per 2–10 fields of view);
F = few (1 specimen per 11–100 fields of view);
R = rare (1 specimen per 101–1000 fields of view);

Estimates of the percentage of nannofossils present in the sediment were made from smear slides using the following scale:

A = abundant (>50%);
C = common (between 10% and 50%);
F = few (between 1% and 10%);
R = rare (<1%);
B = barren (none).

Radiolarians

The radiolarian zonation used on Leg 134 is that described by Sanfilippo et al. (1985), with the relationship to the calcareous nannofossil zonation of Martini (1971) indicated by Bolli et al. (1985, p. 6 and 7). Order-of-magnitude estimates are given, for the total number of radiolarians on a slide as follows:

A = abundant (tens of thousands);
C = common (thousands);
F = few (hundreds);
R = rare (tens);
X = very rare (<10).

Planktonic Foraminifers

The age determination of the Cenozoic sequences is based on planktonic foraminiferal "P" and "N" zonal scheme established by Blow (1969, 1979). However, the Neogene "N" zones applied in this study follow the amended scheme of Kennett and Srinivasan (1983). The datum levels of species outlined by Berggren et al. (1985a, 1985c) are employed here, unless otherwise stated, for the recognition of zonal boundaries.

The taxonomy of the Neogene and Eocene-Oligocene index species is in accordance with the schemes proposed by Kennett and Srinivasan (1983) and Bolli and Saunders (1985), respectively.

Approximately 10 cm^3 of calcareous pelagic sample was disaggregated in a solution of boiling water with added detergent or Calgon. The residues were washed on a 63-μm sieve and dried under a heat lamp. The sand-sized sediment fraction was examined under a stereomicroscope. Assemblages of planktonic foraminifers were selectively "picked" from each productive sample and subsequently mounted on a micropaleontological slide using gum tragacanth.

The relative abundance of species in an assemblage was based on a visual estimate of the >63-μm sediment fraction. The following letters are used to indicate abundance:

A = abundant (>10 specimens per field of view);
C = common (1–10 specimens per field of view);
F = few (1 specimen per 2–10 fields of view);
R = rare (1 specimen per >10 fields of view);
B = barren (no planktonic foraminifers).

The state of preservation of planktonic foraminifers is described as follows:

G = good (little or no fragmentation, overgrowth, and/or dissolution);
M = moderate (some signs of fragmentation, overgrowth, and/or dissolution);
P = poor (severe fragmentation, heavy overgrowth, and/or dissolution).

Larger Benthic Foraminifers

The larger benthic foraminifers were used to determine the ages of neritic carbonate sediments by applying the T-letter zonation scheme as proposed by Adams (1984). For identification of species, specimens were mounted at various orientations in lakeside cement and thin-sectioned to reveal internal structures.

Paleoenvironmental Analysis

In addition to biostratigraphic applications, microfossils were used for paleobathymetric estimates. Where applicable, relative paleodepth evaluations were made using both planktonic and benthic foraminifers.

Smaller Benthic Foraminifers

Smaller benthic foraminifers were used primarily as paleoenvironmental indicators of both the paleodepth and the early geochemical conditions at the water-sediment interface. Approximately 10 cm^3 of sediment sample was used from each core catcher. Carbonate-sand samples were disaggregated in boiling water with added detergent (Calgon); siltstone samples were disaggregated in a weak solution of hydrogen peroxide and Calgon. The residues were washed on a 63-μm sieve and dried under a heat lamp. Smaller benthic foraminifers were examined from the >125-μm fraction. The conventions for describing abundance and preservation of benthic foraminifers are similar to those applied to planktonic foraminifers.

Paleobathymetric interpretations of smaller benthic foraminifers were primarily based on Akimoto's (1990) depth zonations. Where applicable, additional information was obtained from planktonic foraminifers applying the depth zonation of Keller (1985). Bathymetric ranges are as follows: sublittoral (0–150 m) is divided into upper (0–30 m), middle (30–80 m), and lower (80–150 m) parts; bathyal is divided into upper (150–500 m), middle (500–2000 m), and lower (2000–3000 m) parts; and abyssal indicates a depth >3000 m.

PALEOMAGNETISM

Paleomagnetic studies performed aboard the *JOIDES Resolution* during Leg 134 included routine measurements of natural remanent magnetism (NRM) and of magnetic susceptibility of sedimentary and volcanic material. Because cores

are commonly affected by secondary magnetizations, alternating field (AF) demagnetizations were also performed systematically. Where magnetic cleaning successfully isolates primary component of remanence, paleomagnetic inclinations are used to assign a magnetic polarity to the stratigraphic column. With the assistance of biostratigraphic data, polarity reversal zones are correlated with the magnetic polarity time scale of Berggren et al. (1985b) (see "Biostratigraphy" section, this chapter). In addition, magnetic logging involving the measurement of *in-situ* susceptibility and total magnetic field was performed during Leg 134.

Remanent Magnetization Measurements

The *JOIDES Resolution* maintained two magnetometers for measurement of magnetic remanence during Leg 134, a Molspin spinner magnetometer and a 2-G Enterprises (model 760R) pass-through cryogenic superconducting rock magnetometer. An AF demagnetizer (model 2G600) capable of alternating fields up to 20 mT is on-line with the cryogenic magnetometer. Both the cryogenic magnetometer and the AF coils are encased in a Mu-metal shield, and an automated sample-handling system moves the core sections through the AF coils and the magnetometer sensor region. The cryogenic magnetometer, AF demagnetizer, and sample-drive system are controlled by a multiserial communication board (FASTCOM 4) in an IBM PC AT-compatible computer. Measurements using the cryogenic magnetometer were controlled by a modified version of a University of Rhode Island BASIC program. Prior to drilling, we conducted various calibration experiments to establish the accuracy of the basic measurement apparatus and to check the operation of the processing software. In particular, we investigated the possible inversion of the orientation of axes reported during Leg 133 and modified the software controlling the cryogenic magnetometer accordingly.

The superconducting quantum interference device (SQUID) sensors in the cryogenic magnetometer measure magnetization over an interval approximately 20 cm long. The widths of the sensor region suggest that as much as 150 cm^3 of core contributes to the output signal. The large volume of core material within the sensor region allows accurate determination of remanence for weakly magnetized samples despite the relatively high background noise related to the motion of the ship. The cryogenic magnetometer is incapable of measuring archive halves with magnetizations greater than 1 A/m; intensities of this magnitude exceed the sensing range of the cryogenic magnetometer.

The output from the cryogenic magnetometer during continuous measurement assumes a uniformly magnetized core and provides reliable directional data when an interval larger than the sensing region is measured. Tests conducted during Leg 131 indicate that in cases where the core is not uniformly magnetized, either through natural processes or artifacts (voids in the core or differential rotation of segments within the core liner), the values of declination, inclination, and intensity should be treated with caution.

Remanence measurements of sediments and rocks were performed by passing continuous archive-half core sections through the cryogenic magnetometer. NRM measurements were taken at intervals of either 5 or 10 cm along the core, and after AF demagnetization at 5, 10, and 15 mT. The maximum AF demagnetizing field allowed by the Information Handling Panel for archive-half sections is 15 mT or the median destructive field, whichever is lower. In some cores, this field is insufficient to remove secondary remanences and isolate the primary component of remanence required for magnetostratigraphy and plate history. Therefore, at least one discrete shipboard paleomagnetic sample was taken from each section and from each representative lithology. These samples were demagnetized using either a Schonstedt GSD-1 AF demagnetizer capable of fields up to 100 mT or a Schonstedt thermal demagnetizer.

Discrete samples in soft sediment were taken using oriented standard plastic sampling boxes (7 cm^3). In order to reduce the deformation of the sediment, the core was cut using a thin stainless steel spatula before pressing the plastic sampling boxes into the sediment. Minicores were drilled from lithified sedimentary rocks and igneous rocks using a water-cooled nonmagnetic drill bit attached to a standard drill press.

During AF demagnetization of the discrete samples with the GSD-1 AF demagnetizer, we noticed that several samples acquired spurious magnetizations above 40 mT. A few tests were made after demagnetization along each positive and negative axis and the spurious magnetizations were shown to be the sum of two types: an anhysteretic remanence (ARM) produced along the axis of demagnetization and a sample-dependent component of gyromagnetic origin (GRM) that was produced mostly orthogonal to the axis of demagnetization. The acquisition of gyromagnetic remanence during static three-axis AF demagnetization is often not recognized by paleomagnetists and is often confused with ARM acquisition. Detailed descriptions on how to recognize these spurious magnetizations have been given by Dankers and Zijderveld (1981) and Roperch and Taylor (1987).

Perturbations Produced by Drilling

Interpretations of measurements with the pass-through cryogenic magnetometer often are difficult because of mechanical disturbances, such as twisting of unconsolidated sediments during XCB or RCB coring. A persistent problem is the pervasive overprint produced by drilling, as noted on previous legs. Exposure to large magnetic fields on the rig floor and contamination by rust have often been suggested as sources for these spurious magnetizations. During Leg 115, Schneider and Vandamme (Shipboard Scientific Party, 1988) suggested that one particular source of remagnetization was the remanent field of the core barrel.

We performed several tests to establish the nature of spurious magnetizations observed in cores recovered on Leg 134. Low-coercivity sediments at all sites showed strong NRM intensities and steep negative inclinations when archive halves were measured using the cryogenic magnetometer. Discrete samples taken from the center of the working-half sections did not show as strong an overprint, which suggested that the intensity of the overprint decreased radially from the edge to the center of the core. Three discrete samples were taken and demagnetized to test this hypothesis: one from the center of the core, one from the edge, and one from in between (Fig. 8). The primary magnetization in the sample taken from the center was isolated by AF demagnetization at 5 mT. Isolation of the primary component of remanence in the sample taken from the outer edge of the core, however, required AF demagnetization at 15 mT. This drilling-induced overprint may be considered a viscous remanence or may be compared to a strong-field (10–15 mT) isothermal remanent magnetization. Cores recovered using both rotary and piston drilling are affected by this overprint, the intensity of which is dependent upon the magnetic mineralogy of the recovered material.

Magnetic Susceptibility Measurements

Whole-core magnetic susceptibility measurements were made on all APC and selected XCB and RCB cores using a Bartington Instruments magnetic susceptibility meter (model MS1) with an MS1/CX 80-mm whole-core sensor loop set at

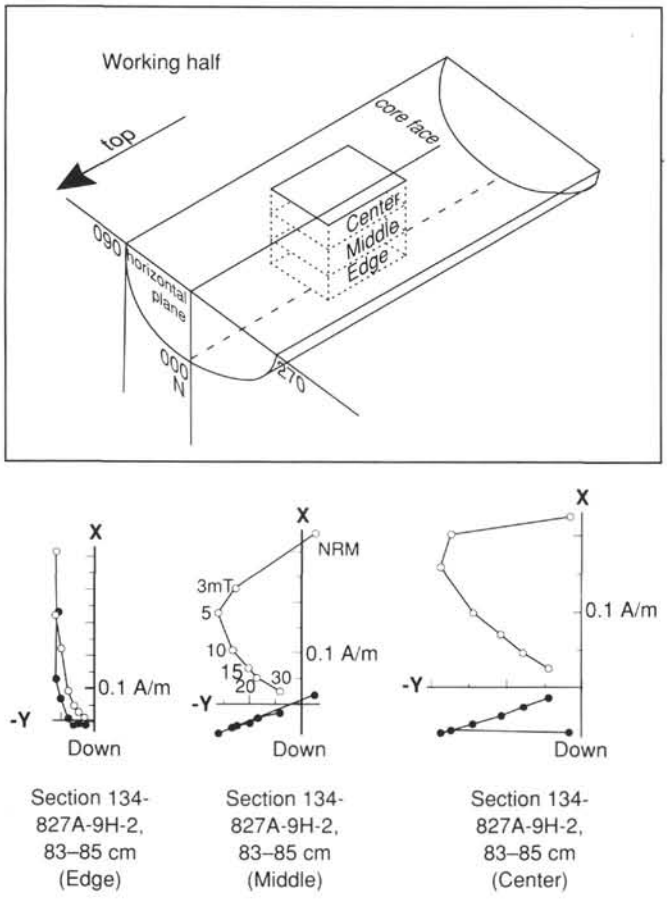

Figure 8. Orthogonal projections of alternating field (AF) demagnetization data from three specimens from Core 134-827A-9H. Open circles correspond to projection onto the vertical plane and solid circles are projections onto the horizontal plane. All three samples were demagnetized using the same AF steps.

0.47 kHz. The susceptibility meter is part of the multisensor track (MST) which also contains a GRAPE and *P*-wave logger (see "Physical Properties" section, this chapter).

The general trend of the susceptibility data curve was used to characterize the magnetic material contained within the cored sediment. The susceptibility response is a function of the mineralogy (on Leg 134, predominantly magnetite) as well as the shape and volume of the magnetic particles within the rocks. Because magnetic susceptibility is a temperature-dependent property, the cores were permitted to equilibrate thermally (2–4 hr) prior to the analysis on the MST.

Downhole Magnetic Measurements

Two magnetic logging tools compatible with Schlumberger and ODP requirements have been manufactured by a research group from France (LETI-CEA) and the oil industry (Total-CFP). One is a susceptibility tool and the other measures the total field. The susceptibility tool consists of a cylinder, 60 mm in diameter and 2.7 m long, that contains the sensor (mutual inductance bridge with two main coils) and electronic circuits. The volume of rocks measured is approximately equivalent to that of a cylinder 0.5 m in radius and 1.5 m in length. The total-field instrument measures the resonance frequency of protons placed in a magnetic field. The resolution of the sensor is 0.01 nT.

Table 3. Shipboard pore-fluid analytical methods.

Analysis	Technique	Units
Salinity	Goldberg refractometer	None
Alkalinity	Gran titration	Millimolar (mM)
pH	TRIS-BIS buffers	[a]pmH
Chlorinity	Mohr titration	Millimolar (mM)
Potassium	Atomic emission spectrometry	Millimolar (mM)
Sodium	Atomic emission spectrometry/ calculated	Millimolar (mM)
Calcium	EGTA titration/atomic absorption spectrometry	Millimolar (mM)
Magnesium	EDTA titration/atomic absorption spectrometry	Millimolar (mM)
Ammonia	Colorimetry	Micromolar (μM)
Phosphate	Colorimetry	Micromolar (μM)
Silica	Colorimetry	Micromolar (μM)

[a] See Gieskes and Gamo (in press).

The total measured field is the sum of the field of internal origin from the earth's core, the external field that results primarily from solar activity, and the field produced by the induced and remanent magnetizations of the rocks measured. The induced contribution was calculated from the susceptibility data. The diurnal variations of the earth's magnetic field were recorded by a reference station operated on Espiritu Santo Island, about 50 km from the drill sites.

The effect of variations of the external field can therefore be determined and subtracted from downhole measurements. A qualitative interpretation of the *in-situ* magnetostratigraphy can be made following guidelines from theoretical investigations of magnetic fields in boreholes (Pozzi et al., 1988).

SEDIMENT AND FLUID GEOCHEMISTRY

Inorganic Geochemistry

Sediment and pore-fluid samples were measured for a variety of chemical components during Leg 134 in order to (1) document diagenetic processes that alter pore-fluid chemistry and (2) identify the fluids that may be flowing or may have flowed through the sediments. Diagenesis and fluid flow are two important processes at convergent margins because of the combination of high concentrations of chemically reactive sedimentary components, such as volcanic ash, and large amounts of tectonic deformation. The types of pore-fluid measurements are listed in Table 3 and the sediments were measured for their organic and inorganic carbon contents. The inorganic carbon contents are plotted against depth in the "Lithostratigraphy" section of each site chapter in this volume.

Pore-Fluid Chemistry

Previous drilling (Mascle et al., 1988; Shipboard Scientific Party, 1991) indicates that structural and lithologic boundaries may control the hydrology at convergent margins. The results at Sites 827 and 828 indicate that structural features are alsoimportant in the New Hebrides Island Arc, and that one sample collected every third core (about every 30 m) would be insufficient to observe subtle changes in the pore-fluid chemistry. All subsequent sites were thus sampled more frequently, at a maximum density of one per every second core (about

Table 4. Leg 134 sample dilutions from alkalinity measurements.

Hole	Core, section, interval (cm)	Depth (mbsf)	Sample volume (cm^3)	Acid volume (cm^3)	Dilution (total/sample)
827A	1H-4, 145–150	6.0	4.8504	1.070	1.2206
	3H-4, 145–150	25.3	4.8504	0.900	1.1856
	6H-4, 145–150	50.9	4.8504	1.346	1.2775
	9H-2, 145–150	70.0	4.8504	1.027	1.2117
	13H-2, 135–140	90.8	4.8504	0.196	1.0404
827B	2R-3, 145–150	122.1	4.8504	Not recorded	
	5R-2, 140–150	149.5	4.8504	0.099	1.0204
	11R-1, 135–150	205.9	4.8504	0.057	1.0118
	14R-2, 0–30	236.3	4.8504	0.106	1.0219
828A	1H-2, 145–150	3.0	4.8504	Sample spilled	
	3H-3, 145–150	18.4	4.8504	0.742	1.1530
	6H-3, 145–150	46.9	4.8504	0.477	1.0983
	9H-5, 145–150	76.9	4.8504	0.194	1.0400
828B	1R-3, 135–150	94.4	4.8504	1.440	1.2969
829A	1R-1, 146–150	1.5	4.8504	0.394	1.0812
	3R-2, 145–150	15.3	4.8504	0.547	1.1128
	5R-5, 145–150	38.5	4.8504	0.346	1.0713
	7R-1, 145–150	52.3	4.8504	0.208	1.0429
	12R-5, 140–150	104.9	4.8504	0.806	1.1662
	14R-4, 135–150	124.1	4.8504	0.685	1.1412
	16R-4, 135–150	143.4	4.8504	0.474	1.0977
829B	2H-2, 145–150	3.5	4.8504	0.435	1.0897
829C	1H-2, 145–150	3	4.8504	0.443	1.0913
	1H-4, 145–150	6	4.8504	0.541	1.1115
	2H-2, 145–150	9.8	4.8504	0.330	1.0680
	3H-6, 135–140	26.8	4.8504	0.480	1.0990
830A	1H-3, 145–150	4.5	4.8504	0.282	1.0581
	3H-4, 145–150	22.5	4.8504	0.160	1.0330
	5H-1, 145–150	36.4	4.8504	0.188	1.0388
830B	4R-1, 100–110	78.5	4.8504	0.140	1.0289
	6R-1, 134–150	98.4	4.8504	0.142	1.0293
	8R-1, 134–150	117.8	4.8504	0.166	1.0342
	10R-2, 0–19	141	4.8504	0.154	1.0317
	12R-2, 0–18	156.8	4.8504	0.134	1.0276
830C	12R-2, 28–53	341.2	4.8504	0.093	1.0192
831A	1H-2, 145–150	3.0	4.8504	0.248	1.0511
831B	5R-3, 145–150	135.4	4.8504	0.244	1.0503
832A	1H-3, 145–150	4.5	4.8504	0.353	1.0728
	4H-3, 145–150	23.0	4.8504	1.295	1.2670
	6H-3, 145–150	42.0	4.8504	1.506	1.3105
	8H-2, 144–150	59.5	4.8504	1.604	1.3307
	10H-3, 143–150	77.0	4.8504	1.601	1.3301
	16H-3, 145–150	117.5	4.8504	1.464	1.3018
	19H-1, 145–150	142.5	4.8504	1.415	1.2917
	24H-2, 145–150	180.7	4.8504	1.179	1.2431
832B	9R-2, 140–150	222.9	4.8504	0.635	1.1309
	15R-2, 58–68	280.0	4.8504	0.104	1.0214
	17R-1, 10–20	300.3	4.8504	0.098	1.0202
	19R-1, 140–150	319.5	4.8504	0.092	1.0190
	23R-2, 16–31	358.2	4.8504	0.090	1.0186
	28R-2, 135–150	407.8	4.8504	0.113	1.0233
	30R-4, 138-150	428.0	4.8504	0.108	1.0223
	32R-2, 135–150	445.8	4.8504	0.103	1.0212
	34R-1, 135–150	462.9	4.8504	0.106	1.0219
	37R-3, 130–150	494.7	4.8504	0.108	1.0223
	42R-2, 0–13	540.4	4.8504	0.108	1.0223
	45R-1, 130–150	569.0	4.8504	0.107	1.0221
	47R-1, 130–150	588.3	4.8504	0.099	1.0204
	49R-CC, 0–20	611.2	4.8504	0.096	1.0198
	61R-2, 130–150	723.6	4.8504	0.075	1.0155
	63R-6, 0–20	747.3	4.8504	0.089	1.0183
833A	1H-3, 145–150	4.5	4.8504	0.799	1.1647
	3H-3, 145–150	23.5	4.8504	1.094	1.2255

Table 4 (continued).

Hole	Core, section, interval (cm)	Depth (mbsf)	Sample volume (cm^3)	Acid volume (cm^3)	Dilution (total/sample)
833A	6H-1, 145–150	40.7	4.8504	0.935	1.1928
	8H-1, 145–150	55.5	4.8504	0.811	1.1672
	10H-4, 145–150	68.9	4.8504	0.751	1.1548
	13H-1, 145–150	79.5	4.8504	0.5244	1.1081
	16H-2, 140–150	95.6	4.8504	0.186	1.0383
	21X-2, 140–150	144.9	4.8504	0.128	1.0264
	23X-2, 0–10	162.8	4.8504	0.158	1.0326
	26X-1, 92–102	191.2	4.8504	0.117	1.0241
833B	5R-2, 90–101	118.2	4.8504	0.109	1.0225
	14R-3, 140–150	207.2	4.8504	0.114	1.0235
	16R-1, 140–150	223.5	4.8504	0.1	1.0206
	18R-1, 141–150	242.3	4.8504	0.093	1.0192
	20R-1, 140–150	261.4	4.8504	0.077	1.0159
	22R-2, 0–10	280.8	4.8504	0.081	1.0167
	25R-1, 95–105	309.2	4.8504	0.085	1.0175
	27R-1, 136–150	328.9	4.8504	0.083	1.0171
	29R-1, 117–131	348.1	4.8504	0.091	1.0188
	31R-2, 135–150	369.1	4.8504	0.078	1.0161
	33R-1, 112–125	386.3	4.8504	0.085	1.0175
	46R-3, 135–150	494.5	4.8504	0.072	1.0148
	63R-2, 0–15	656.4	4.8504	0.074	1.0153

every 20 m). In many lithologies, however, limited core recovery dictated a smaller sampling density. The first samples taken at each site were 5-cm lengths of the whole-round core, but the length of samples increased to 35 cm as the sediments became more indurated with depth. The amount of fluid obtained per centimeter of core is plotted against depth in the site chapters. This value is only a qualitative estimate of the fluid contained within the sediment because the core diameters vary depending on the coring technique and because pore fluids were not extracted from those parts of the core that were disturbed by drilling.

After the cores were brought on deck, each sample was collected before the end caps were sealed with acetone. The samples were cleaned, by scraping with a stainless steel spatula, of material that appeared to be contaminated by the fluids used as drilling mud, particularly in fractures and along the outside edge of the sample. The whole-round samples were squeezed in high-pressure stainless steel presses (Manheim and Sayles, 1974). The maximum pressure used was about 30,000 pounds per square inch (psi) (2.11×10^7 kg/m^2) and pressure was applied until no additional fluid was obtained. The samples were squeezed as soon as possible after recovery but they generally had equilibrated to room temperature prior to the squeezing procedure. Because *in-situ* temperatures varied from 2° to ~50°C, the change in temperature may produce some artifacts (Sayles et al., 1973; Gieskes, 1973, 1974), but overall trends and concentration variations in neighboring cores should not be altered. All samples were filtered through 0.45-μm Gelman acrodisc disposable filters and subsequently subdivided for both shipboard work as well as for future work in shore-based laboratories.

The procedure for each analysis (Table 3) is described by Gieskes and Gamo (in press) and references therein. The alkalinity was titrated using Baker "Ultrex" ultrapure HCl because the alkalinity samples from Legs 112 and 131 were found to be contaminated by high concentrations of iodine in the acid (Gieskes and Gamo, in press). Table 4 shows the volumes of sample and acid used for each titration and the dilution caused by addition of acid to the sample. The alkalinity samples were sealed in polyethylene tubes immediately following the titration and thus should be useful for any subsequent chemical analysis.

Sediment Chemistry

Inorganic carbon contents were routinely measured in splits of the samples that had been used for the physical properties studies and this value was used to calculate the percentage by weight of $CaCO_3$ in the samples. The measurements were made using a Coulometrics 5011 coulometer equipped with a System 140 carbonate carbon analyzer. Depending on carbonate content, 15 to 70 mg of ground and

weighed sediment was reacted in a 2-N HCl solution. The liberated CO_2 was titrated in a monoethanolamine solution with a color indicator, whereas the change in light transmittance was monitored with a photo-detection cell.

Organic Geochemistry

Shipboard organic geochemistry was measured during Leg 134 in order to monitor volatile hydrocarbon concentrations for safety reasons. Hydrocarbon concentrations appear to characterize fluids within décollement zones (Gieskes et al., 1990a, 1990b) and thus the hydrocarbon concentrations were also used as tracers for flow of deep-seated fluids. The sedimentary organic carbon component was measured to provide an initial characterization of the content of organic matter.

Elemental Analyses

Total nitrogen, carbon, and sulfur concentrations were measured on oven-dried samples of the sediment residues from the physical properties measurements using a NA 1500 Carlo Erba NCS analyzer. The bulk samples plus vanadium pentoxide were combusted at 1000°C in an oxygen atmosphere, converting organic and inorganic carbon into CO_2 and sulfur into SO_2. These gases along with nitrogen were then separated by gas chromatography and measured with a thermal conductivity detector (TCD). The total organic carbon (TOC) content of the sediments was calculated by subtraction of the inorganic carbon content from the total carbon content. Because of the low organic carbon contents and difficulty with the instrument, the Rock-Eval procedure was not used.

Gas Analyses

Gases were extracted from bulk sediments utilizing headspace sampling techniques (Emeis and Kvenvolden, 1986). A ~5-cm^3 plug of sediment was taken as the core arrived on deck, utilizing a No. 4 cork borer. The sample was placed immediately in a glass vial that subsequently was sealed with a septum and metal crimp and than heated to 70°C and kept at this temperature for 45 min.

Each gas sample was expanded into a gas-tight syringe and injected into an HP 5890A NGA gas chromatograph for flame ionization detection (FID) and TCD analyses. The gas chromatographic system employs a steel column (6 in. × 1/8 in.) packed with Poropak T, a steel column (3 ft × 1/8 in.) with a 13X molecular sieve, a steel column (6 ft × 1/8 in.) packed with 80/100 mesh Hayesep R(AW), and a DB1 (1-mm film thickness, J&W). Appropriate automatic valve switching, controlled by a HP 3392 integrator that also recorded and integrated the count rates, provided a rapid determination of oxygen, nitrogen, carbon dioxide, and hydrocarbons from methane to hexanes. The separation on the FID line was carried out isothermally at 40°C at a flow rate of 2.24 cm^3/min. Helium was used as carrier gas. All gas concentrations are reported in parts per million (ppm).

IGNEOUS ROCKS

Core Curation and Shipboard Sampling

In order to preserve important features and structures, core sections containing igneous rocks were examined prior to splitting with a diamond saw into archive and working halves. During core handling and splitting, care was taken to ensure that the core orientation was preserved by marking the original base of individual pieces. Each piece was numbered sequentially from the top of each core section and labeled at the top surface. Pieces that could be fitted together were assigned the same number, but were lettered consecutively (e.g., 1A, 1B, and 1C). Plastic spacers were placed only between pieces with different numbers. The presence of a spacer, therefore, may represent a substantial interval of no recovery. If it was evident that an individual piece had not rotated about a horizontal axis during drilling, an arrow was added to the label pointing to the top of the section. As pieces were free to turn about a vertical axis during drilling, azimuthal orientation of a core was not possible.

After the core was split, the working half was sampled for shipboard physical properties, magnetic studies, X-ray fluorescence, X-ray diffraction, and thin-section studies. Nondestructive physical properties measurements, such as magnetic susceptibility, were made on the archive half of the core. Where recovery permitted, samples were taken from each lithologic unit. Some of these samples were minicores. The archive half was described on the visual core description form and was photographed before storage.

Visual Core Descriptions

Visual core description (VCD) forms were used in the documentation of the igneous rock cores (see VCD forms following the core barrel sheets in the back of this volume). The left column is a graphic representation of the archive half. A horizontal line across the entire width of the column denotes a plastic spacer. Oriented pieces are indicated on the form by an upward-pointing arrow to the right of the piece. Shipboard samples and studies are indicated in the column headed "shipboard studies," using the following notation: XD = X-ray diffraction analysis; XF = X-ray fluorescence analysis; TS = petrographic thin section; PP = physical properties analysis; and PM = paleomagnetic analysis.

To ensure consistent and complete documentation, the visual core descriptions were entered into the computerized database HARVI. The database is organized into separate data sets for fine-grained rocks and coarse-grained rocks. Each record is checked by the database program for consistency and is printed in a format that can be directly pasted onto the barrel sheet for subsequent curatorial handling.

When describing sequences of rocks, the core was subdivided into lithologic units on the basis of changes in petrography, mineral abundances, rock composition, and rock clast type. For each lithologic unit and section, the following information was recorded in the database system:

1. The leg, site, hole, core number, core type, and section number.
2. The unit number (consecutive downhole), position in the section, number of pieces of the same lithologic type, the rock name, and the identity of the describer.
3. The dry color of the rock and the presence and character of any deformation.
4. The number of mineral phases visible with a hand lens and their distribution within the unit, together with the following information for each phase: (1) abundance (volume percent), (2) size range in millimeters, (3) shape, (4) degree of alteration, and (5) further comments.
5. The groundmass texture: glassy, fine-grained (<1 mm), medium-grained (1–5 mm), or coarse-grained (>5 mm). Relative grain size changes within the unit were also noted.
6. The presence and characteristics of secondary minerals and alteration.
7. The abundance, distribution, size, shape, and infilling material of vesicles (including the proportion of vesicles that are filled by alteration minerals).
8. The structure, including any layering and noting whether the flow is massive, pillowed, thin or sheetlike, brecciated, or a hyaloclastite.

9. The relative amount of rock alteration: fresh (<2%), slightly altered (2%–10%), moderately altered (10%–40%), highly altered (40%–80%), very highly altered (80%–95%), and completely altered (95%–100%). The type, form, and distribution of alteration was also noted.

10. The presence of veins and fractures, including their abundance, width, and orientation. Orientation of veins and fractures was measured with a protractor such that the top of each core is considered 0°. The relationship of the veins and fractures to the alteration and filling was also noted.

11. Other comments, including notes on the continuity of the unit within the core and on the interrelationship of units.

Basalts and diabases are termed aphyric (<1%), sparsely phyric (1%–2%), moderately phyric (2%–10%), or highly phyric (>10%), depending upon the proportion of phenocrysts visible with a hand lens or binocular microscope. Basalts are further classified by phenocryst type (e.g., a moderately plagioclase-olivine phyric basalt contains 2%–10% phenocrysts, mostly plagioclase, with subordinate olivine). Volcanic rock names were initially assigned from megascopic phenocryst assemblages. Where chemical analyses or thin sections became available, more specific rock names were given.

Igneous visual core descriptions are presented in the back of this volume, and descriptions of each rock unit from Leg 134 are available from the computerized database at the ODP Gulf Coast Repository.

Thin-Section Descriptions

Thin sections of igneous rocks were examined to complement and refine the hand-specimen observations. The percentages and textural descriptions of individual phases were reported in the computerized database HRTHIN. The terminology used for thin sections was the same as that applied in the megascopic descriptions. Thin-section descriptions are included in the VCD forms and are also available from the ODP computerized database.

X-ray Diffraction Analyses

A Philips ADP 3520 X-ray diffractometer was used for the XRD analysis of mineral phases. CuKα radiation was measured through a Ni filter at 40 kV and 35 mA. The goniometer scanned from 2° to 70° 2Θ with a step size of 0.02°, and the counting time was 1 s per step. However, because of a technical problem peaks below 10° were not well resolved, which made identification of layered silicate minerals difficult.

Samples were ground in a Spex 8000 Mixer Mill or an agate pestle and mortar. The powder was then pressed into the sample holders or smeared on glass plates for analysis. Diffractograms were interpreted with the help of a computerized search and match routine using the Joint Committee on Powder Diffraction Standards powder files.

X-ray Fluorescence (XRF) Analysis

Prior to analysis, samples were crushed in a Spex 8510 shatterbox using a tungsten carbide barrel. This produces some Ta and massive W contamination, so that the powder is unsuitable for instrumental neutron activation (INNA) analysis.

A fully automated wavelength-dispersive ARL8420 XRF (3 kW) system equipped with a Rh target X-ray tube was used to determine the major oxide and trace element abundances of whole-rock samples. Analyses of the major oxides were carried out on lithium borate glass disks doped with lanthanum as a "heavy absorber" (Norrish and Hutton, 1969). The disks were prepared from 500 mg of rock powder, ignited for 2 hr at about 1030°C, and mixed with 6.000 g of dry flux consisting of 80% lithium tetraborate and 20% La_2O_3. This mixture was then melted in air at 1150°C in a Pt-Au crucible for about 10 min and poured into a Pt-Au mold using a Claisse Fluxer. The 12:1 flux to sample ratio and the use of the lanthanum absorber made matrix effects insignificant over the normal range of igneous rock compositions. Hence the relationship between X-ray intensity and concentration becomes linear and can be described by

$$C_i = (I_i \times m_i) - b_i, \quad (1)$$

where C_i = concentration of oxide i (weight percent, or wt%); I_i = net peak X-ray intensity of oxide i; m_i = slope of calibration curve for oxide i (wt%/cycles per second); and b_i = apparent background concentration for oxide i (wt%).

The slope m_i was calculated from a calibration curve derived from the measurement of well-analyzed reference rocks (BHVO-1, G-2, AGV-1, JGB-1, JP-1, BR, and DRN). The background b_i was determined either on blanks or derived by regression analysis from the calibration curves.

Systematic errors resulting from short-term or long-term fluctuations in X-ray tube intensity were corrected by normalizing the measured intensities of the samples to those of a standard that was always run together with a set of six samples. To reduce shipboard weighing errors, two glass disks were prepared for each sample. Accurate weighing was difficult on board the moving platform of the *JOIDES Resolution* and was performed with particular care, as weighing errors could be a major source of imprecision in the final analysis. Loss on ignition values were determined by drying the sample at 110°C for 8 hr, and then by weighing before and after ignition at 1030°C in air.

Trace-element determinations were made on pressed-powder pellets prepared by pressing (with 7 tons of pressure) a mixture of 5.0 g of dry rock powder (dried at 110°C for >2 hr) and 30 drops of polyvinyl alcohol binder into an aluminum cap. A modified Compton scattering technique based on the intensity of the Rh Compton peak was used for matrix absorption corrections (Reynolds, 1967).

Replicate analyses of rock standards show that the major element data are precise within 0.5% to 2.5%, and are considered accurate to ~1% for Si, Ti, Fe, Ca, and K, and between 3% and 5% for Al, Mn, Na, and P. The trace-element data are considered accurate between 2% and 3% or 1 ppm (whichever is greater) for Rb, Sr, Y, and Zr, and between 5% and 10% or 1 ppm for the others, except for Nb, Ba, and Ce. Precision is also within 3% for Ni, Cr, and V at concentrations >100 ppm, but 10% to 25% at concentrations <100 ppm. Analytical conditions for the XRF analyses are given in Table 5.

DOWNHOLE MEASUREMENTS

Tool Strings

Downhole logging directly determines physical and chemical properties of formations adjacent to the borehole. Interpretation of these continuous, *in-situ* measurements can yield a stratigraphic, lithologic, geophysical, and mineralogic characterization of the site. After coring is completed at a hole, a tool string is lowered downhole on a seven-conductor cable, and each of several tools in the tool string continuously monitors some property of the adjacent borehole. Three Schlumberger tool strings were used on Leg 134: the geophysical, geochemical, and formation microscanner (FMS) combinations. The Lamont-Doherty Geological Observatory (LDGO) temperature tool was attached to the base of the first two tool strings. The new digital borehole televiewer and the high-resolution magnetometer tool (GHMT) were used at selected sites.

The geophysical tool string combination used on Leg 134 consisted of long-spaced sonic (LSS), natural gamma-ray tool (NGT), high-temperature lithodensity tool (HLDT), mechan-

Table 5. Leg 134 XRF analytical conditions.

Element	Line	Crystal	Detector[a]	Collimator	Peak angle (°)	Background offset (°)	Total count time (s) Peak	Background
SiO_2	Kα	PET(002)	FPC	Coarse	109.10	0	40	0
TiO_2	Kα	LiF(200)	FPC	Fine	86.16	0	40	0
Al_2O_3	Kα	PET(002)	FPC	Coarse	144.49	0	100	0
Fe_2O_3*	Kα	LiF(200)	FPC	Fine	57.53	0	40	0
MnO	Kα	LiF(200)	KrSC	Fine	63.03	0	40	0
MgO	Kα	TLAP	FPC	Coarse	44.88	±0.80	200	400
CaO	Kα	LiF(200)	FPC	Coarse	113.18	0	40	0
Na_2O	Kα	TLAP	FPC	Coarse	54.73	−1.20	200	200
K_2O	Kα	LiF(200)	FPC	Fine	136.66	0	40	0
P_2O_5	Kα	Ge(111)	FPC	Coarse	141.00	0	100	0
Rh	K-C	LiF(200)	Scint	Fine	18.60	0	100	0
Nb	Kα	LiF(200)	Scint	Fine	21.39	±0.35	200	200
Zr	Kα	LiF(200)	Scint	Fine	22.54	±0.35	100	100
Y	Kα	LiF(200)	Scint	Fine	23.83	±0.40	100	100
Sr	Kα	LiF(200)	Scint	Fine	25.15	±0.41	100	100
Rb	Kα	LiF(200)	Scint	Fine	26.60	±0.60	100	100
Zn	Kα	LiF(200)	Scint	Fine	41.81	±0.40	60	60
Cu	Kα	LiF(200)	Scint	Fine	45.02	±0.40	60	60
Ni	Kα	LiF(200)	Scint	Coarse	48.64	±0.60	60	60
Cr	Kα	LiF(200)	FPC	Fine	69.38	±0.50	60	60
Fe	Kα	LiF(220)	FPC	Fine	85.73	−0.40 + 0.70	40	40
V	Kα	LiF(220)	FPC	Fine	123.20	−0.50	60	60
TiO_2	Kα	LiF(200)	FPC	Fine	86.16	±0.50	40	40
Ce	Lα	LiF(220)	FPC	Coarse	128.35	±1.50	100	100
Ba	Lβ	LiF(220)	FPC	Coarse	128.93	±1.50	100	100

Note: *Total Fe as Fe_2O_3. All elements analyzed under vacuum on goniometer 2 at generator settings of 60 kV and 50 mA.

[a] FPC = flow proportional counter using P_{10} gas; KrSC = sealed Krypton gas counter; Scint = NaI scintillation counter.

ical caliper device (MCD), and phasor dual-induction tool (DIT). This tool combination measures compressional wave velocity and provides indicators of the two variables that most often control velocity: porosity, as indicated by density or resistivity, and clay content, as indicated by the natural gamma-ray tool.

The FMS tool string included not only the FMS but also a general purpose inclinometer tool (GPIT) that spatially orients the FMS resistivity image of the borehole wall. The tool string also contained a natural gamma-ray tool (NGT) to allow depth correlation of the FMS data with other logs.

The geochemical combination for Leg 134 consisted of the NGT, aluminum clay tool (ACT), and gamma spectrometry tool (GST). This tool combination measures the relative concentrations of 12 elements: silicon, calcium, aluminum, iron, titanium, sulfur, hydrogen, chlorine, potassium, thorium, uranium, and gadolinium.

Log data are recorded at 0.5-ft (0.15-m) intervals for the standard Schlumberger logging strings. The FMS and borehole televiewer logging strings record data on millimeter-scale vertical intervals.

Logs

A brief description of logging tools run during Leg 134 is presented here. A detailed description of logging tool principles and applications is provided in Schlumberger (1989), Serra (1984, 1989), and Timur and Toksoz (1985).

Electrical Resistivity

The dual induction tool provides three different measurements of electrical resistivity, each with a different depth of investigation. Two induction devices (deep and medium resistivity) send high-frequency alternating currents through transmitter coils, creating magnetic fields that induce secondary (Foucault) currents in the formation. These ground-loop currents produce new inductive signals, proportional to the conductivity of the formation, which are recorded by the receiving coils. Measured conductivities are then converted to resistivity. A third device (spherically focused resistivity) measures the current necessary to maintain a constant voltage drop across a fixed interval. Vertical resolution is around 2 m for the medium and deep resistivity devices and about 1 m for the focused resistivity.

Water content and salinity are by far the most important factors controlling the electrical resistivity of rocks. To the first order, resistivity responds to the inverse square root of porosity (Archie, 1942). Other factors influencing resistivity include the concentration of hydrous and metallic minerals, vesicularity, and the geometry of interconnected pore space.

Sonic Velocity Measurements

The LSS tool uses two acoustic transmitters and two receivers to measure the time required for sound waves to travel over source-receiver distances of 2.4, 3.0, and 3.6 m. The raw data are expressed as time required for a sound wave to travel through 0.31 m of formation (μs/ft); these traveltimes are then converted to sonic velocities. First arrivals for the individual source-receiver paths are used to calculate the velocities of the different waves traveling in the formation (compressional, shear, etc.). Only compressional wave velocity is determined during data acquisition, but waveforms are recorded for post-cruise determination of shear-wave velocities and refining the compressional wave velocities. The vertical resolution of the tool is 0.61 m. Compressional wave velocity is dominantly controlled by porosity and lithification; decreases in porosity and increases in lithification cause the velocity to increase.

Natural Gamma-Ray Tool

The NGT measures the natural radioactivity of the formation. Most gamma rays are emitted by the radioactive isotope ^{40}K and

by the radioactive elements of the U and Th series. The gamma-ray radiation originating in the formation close to the borehole wall is measured by a scintillation detector. The elemental abundances of K, U, and Th are determined by analyzing the gamma-ray spectrum using five discrete energy windows.

Because radioactive elements tend to be most abundant in clay minerals, the gamma-ray curve is commonly used to estimate the clay or shale content. There are rock matrices, however, for which the radioactivity ranges from moderate to extremely high values as a result of the presence of volcanic ash, potassic feldspar, or other radioactive minerals.

Mechanical Caliper Device

The MCD provides a basic two-dimensional caliper log of the borehole by means of a bowspring-mounted measurement system. The hole diameter log is used to detect washouts or constrictions. Borehole diameter significantly affects many of the other logging measurements, and the hole diameter is an important input to log correction routines. This caliper tool is subject to sticking when formation mud gets into its mechanical parts, resulting in bimodal (fully open or nearly fully closed) readings. In contrast, the measurement of hole diameter produced by the HLDT is much more reliable. Consequently, on Leg 134 the MCD tool was used primarily to provide centralization and associated improved log quality for the sonic log rather than to measure hole diameter.

High-Temperature Lithodensity Tool

The HLDT uses a ^{137}Ce gamma-ray source and measures the resulting flux at fixed distances from the source. Under normal operating conditions, attenuation of gamma rays is caused chiefly by Compton scattering (Dewen, 1983). Formation density is extrapolated from this energy flux by assuming that the atomic weight of most rock-forming elements is approximately twice the atomic number. A photoelectric effect index is also provided. Photoelectric absorption occurs at energies below 150 keV and depends on the energy of the incident gamma ray, the atomic cross section, and the nature of the atom. Because this measurement is almost independent of porosity, it can be used directly as an indicator of matrix lithology. The radioactive source-and-detector array is pressed against the borehole wall by a strong spring arm. The extension of this spring arm measures hole diameter. Excessive roughness of the hole will cause some drilling fluid to infiltrate between the detector array and the formation. As a consequence, density readings may be artificially low. Approximate corrections can be applied by using the caliper data. The vertical resolution is about 0.30 m.

Compensated Neutron Porosity Tool (CNT)

A radioactive source mounted on the CNT sonde emits high-energy neutrons (4 MeV) into the formation, where they are scattered and slowed by collisions with atomic nuclei. When the neutrons reach a low energy level (0.025 MeV) they are captured by atomic nuclei such as hydrogen, chlorine, silicon, and boron. The scattering cross section is the quantity that describes the rate at which neutrons are slowed. Because the scattering cross section for hydrogen is about 100 times larger than for any other common element in the crust, most energy dissipation is caused by collisions with water molecules. Therefore, a change in the number of neutrons detected at a receiver may be related to porosity. In practice, an array of detectors is used to minimize borehole or drilling fluid effects. Because water is present both in pores and as bound water (e.g., clay minerals), porosity measurements made in the presence of hydrous minerals overestimate the true porosity. The vertical resolution of the tool is theoretically about 0.25 m, but a low signal-to-noise ratio degrades this potential resolution.

Gamma Spectrometry Tool

The induced spectral gamma-ray tool consists of a pulsed source of 14-MeV neutrons and a gamma-ray scintillation detector. A surface computer performs spectral analysis of gamma rays resulting from the interactions of neutrons emitted by the source with atomic nuclei in the formation (Hertzog, 1979). Characteristic sets of gamma rays from six elements dominate the spectrum, permitting calculation of six elemental yields: calcium, silicon, iron, chlorine, hydrogen, and sulfur. The tool normalizes their sum so that the yields do not reflect the actual elemental composition. Instead, ratios of these yields are commonly used in interpreting the lithology, porosity, and salinity of the formation fluid. Shore-based processing is used to derive elemental composition from this and the other logs.

Aluminum Clay Tool

Aluminum abundance as measured by the ACT is determined by neutron-induced gamma-ray spectrometry using californium as the radioactive source. By placing NaI detectors both above and below the neutron source, contributions from natural gamma-ray activity can be removed. Calibration to elemental weight percent is performed by taking irradiated core samples of known volume and density and measuring their gamma-ray output while placed in a jig attached to the logging tool (generally after logging).

Formation Microscanner

The FMS produces high-resolution microresistivity images or structural maps of the borehole wall that can be used for detailed sedimentological or structural interpretations and for determining fracture and breakout orientations. The tool consists of 16 electrode "buttons" on each of four orthogonal pads that are pressed against the borehole wall. The electrodes are spaced about 2.5 mm apart and are arranged in two diagonally offset rows of eight electrodes each. The focused current that flows from the buttons is recorded as a series of curves that reflect the microresistivity variations of the formation. Onboard or shore-based processing convert the current intensity measurements into complete, spatially oriented images. Further processing can also provide measurements of dip magnitude and direction or azimuth of bedding surfaces.

Applications of the FMS images include detailed correlation of coring and logging depths, orientation of cores, mapping of fractures, faults, foliations, and formation structures, as well as determining strikes and dips of bedding. The FMS can also be used to measure stress in the borehole through breakout delineation. In an isotropic, linearly elastic rock subjected to an anisotropic stress field, breakouts form in the direction of the least principal horizontal stress. An important limitation is the restriction to a hole diameter of less than 37 cm (14.5 in.). Thus, little useful information can be obtained from seriously washed-out sections of hole.

General Purpose Inclinometer Tool

The GPIT provides a measurement of borehole inclination, the orientation of the tool with respect to the earth's magnetic field using a three-component magnetometer, and tool motion using an accelerometer. It is run with the FMS to provide spatial orientation of the borehole wall images.

Borehole Televiewer (BHTV)

The BHTV produces an ultrasonic acoustical image of the borehole wall. A transducer emits ultrasonic pulses that are reflected at the borehole wall and then are received by the same transducer. The amplitude and traveltime of the reflected signal are determined and stored in the logging computer. The 360° rotation of the transducer and the upward motion of the tool produces a complete map of the borehole wall. The amplitude depends on the reflection coefficient of the borehole fluid-rock interface, the position of the BHTV tool in the borehole, the shape of the borehole, and the roughness of the borehole wall. The change of the roughness of the borehole wall (e.g., at fractures intersecting the borehole) is responsible for the modulation of the reflected signal. Thus fractures or changes in character of the drilled rocks can easily be recognized in the amplitude image. The recorded traveltime image gives detailed information about the shape of the borehole: knowing the velocity of the ultrasonic signal in the borehole fluid allows one to calculate the caliper value of the borehole from each recorded traveltime. Typically 128 points are recorded per transducer revolution, therefore the BHTV can be considered a "multi-arm caliper log."

Amplitude and traveltime are recorded together with a reference to magnetic north, which permits proper data orientation. This feature can be used to reorient cores providing that they have features (e.g., fractures) that can be recognized in the BHTV data.

The digital BHTV was first used on the *JOIDES Resolution* during Leg 134. The older analog BHTV has been relegated to backup status.

High-Resolution Magnetometer Tool

The GHMT was also first used on board the *JOIDES Resolution* during Leg 134 as a field test to determine its suitability for ODP use. This tool has two operating modes, each of which requires a separate logging run. The first mode is as a high-resolution (0.1 nT) total-field magnetometer (NMRT). The second mode is as a high-resolution (10^{-9} SI) magnetic susceptibility tool (SUMT).

Water Sampler–Temperature–Pore-Pressure Tool (WSTP)

The WSTP tool has a thin, stainless steel probe that is pushed ahead of the bit into the undisturbed sediments at the bottom of the hole. The instrument can measure either sediment temperature or pore-fluid pressure, and can collect a pore-water sample at a preset time. When configured to measure temperature, the tool consists of a thermistor mounted at the end of the probe, a self-contained recorder, a timer to open the fluid-sampling valve, and a 16-V power supply. In pore-pressure configuration, the instrument is fitted with a hollow probe tipped with a sintered stone, allowing a hydraulic connection between the end of the probe and an absolute pressure transducer. A second transducer is configured to monitor hydrostatic pressure. Pore fluid is collected through a filter block above the probe (Barnes, 1988).

In operation, the WSTP tool is mounted inside a core barrel and lowered down the drill pipe by wireline while the bit is held above the bottom of the hole. The tool is held briefly above mudline to measure reference values of either temperature or pressure. The tool is then lowered and latched into place, with the probe tip extending 1.1 m ahead of the bit. The drill string is lowered and the probe is forced into the bottom. A colleted delivery system allows the probe to retract back up inside the bit should the formation prove to be too hard for penetration. With an APC/XCB bottomhole assembly, the bit can be decoupled from the tool after penetration so that the probe will not be disturbed by drill-string heave.

Penetration of about 70 cm is required within about 3 hr of drilling for the temperature of the formation to be undisturbed by the effects of cold circulation fluid. The thermistor/recording package has a nominal resolution of about 10 ohms, or 0.01°C at 25°C. The relatively short length of the narrow probe appears to allow only a few minutes of undisturbed measurements before a thermal disturbance is conducted down from the larger-diameter section above. This limits the accuracy of temperature extrapolations to about ±0.1°–0.2°C. The pressure transducers have resolution of about 8–10 psi. There is significant disturbance of the formation resulting from insertion of the probe, but as the instrument cannot be left in position to allow this disturbance to decay completely, extrapolation to equilibrium is required. The theory of measurement was given in Erickson et al. (1975). A review of thermal data obtained with this type of probe during the DSDP program is given in Hyndman et al. (1987).

A prototype of the Andara APC shoe temperature tool was tested on Leg 134. This tool is similar in concept to the Von Herzen HPC/APC shoe temperature tool used during the DSDP and on ODP through Leg 116 (Hyndman et al., 1987).

LDGO Temperature Tool

The LDGO temperature tool is a self-contained tool that can be attached to any Schlumberger tool string. Data from two thermistors and a pressure transducer are collected every 0.5–5.0 s and stored in a Tattletale computer within the tool. Following the logging run, data are dumped from the Tattletale to the Masscomp computer for analysis. A fast-response, lower accuracy thermistor is able to detect sudden, very small temperature excursions caused by fluid flow from the formation. A slow-response, higher accuracy thermistor can be used to estimate heat flow, if one knows the history of drilling-fluid circulation in the hole and if one has at least two temperature logs (Jaeger, 1961). Data are recorded as a function of time; conversion to depth can be based on the pressure transducer or, preferably, on simultaneous recording by Schlumberger of both depth and time.

Log Data Quality

The quality of log data may be seriously degraded in excessively large borehole diameter or by rapid changes in the diameter. Resistivity and velocity measurements are less sensitive to borehole effects, whereas the nuclear measurements (density, neutron porosity, and both natural and induced spectral gamma ray) are most seriously impaired because of the large attenuation by the borehole fluid. Corrections can be applied to the original data in order to reduce the effects of these conditions and, generally, any departure from the conditions under which the tool was calibrated.

Different logs may have small depth mismatches, caused by either cable stretch or ship heave during recording. Small errors in depth matching can impair the results in zones of rapidly varying lithology. To minimize such errors, a hydraulic heave compensator adjusts for rig motion in real time. In zones of low core recovery, the depth of logs cannot be matched precisely to that of cores because of the inherent ambiguity of placing the recovered section within the interval cored. Accurate depth matching requires a characteristic property of the core that can be measured both on the recovered core and with the downhole logs.

Log Analysis

During logging, incoming data are observed in real time on a monitor oscilloscope and simultaneously recorded on digital tape or disc in the Schlumberger logging unit. After logging, the Schlumberger tapes are read by the Masscomp computer system or the Vaxstation 3200 in the downhole measurements laboratory and reformatted to a file format compatible with the Terralog log-interpretation software package. Rather than being a "black box," Terralog is an interactive system consisting of many log manipulation and plot options. Thus, the log analysis and interpretation varies in duration and procedure for each site. Most log interpretation is carried out aboard ship; further analysis and interpretation are performed after the cruise, using a companion system in the LDGO Borehole Research Laboratory. The most comprehensive reworking of the log data is for the geochemical logs, which are integrated with the other logs and completely recalculated. This permits us to calibrate the log data to the analyses of recovered core samples.

Synthetic Seismograms

Synthetic seismograms are generated from logging data obtained with the LSS tool. The bulk density log from the lithodensity tool or a pseudodensity log created from other logs is required in addition to the slowness log. In many cases, a simple constant density log can be utilized. Experience shows that this often gives surprisingly good results because both velocity and density are usually controlled by the same parameter, porosity. When velocity and density are highly correlated, synthetic seismograms using a constant density log or an actual density log are virtually identical.

The slowness and density logs are used in a program which generates an impedance log (velocity × density) that is convolved with a zero-phase Ricker or other assumed wavelet. The frequency of this wavelet can vary depending on the source that generated the original seismic profile. A 30-Hz wavelet is capable of a vertical resolution on the order of 30 m, so reflectors cannot generally be attributed to any small-scale lithologic horizons. The synthetic seismogram is calculated on the basis of convolutional model, with interbed multiples.

STRUCTURAL STUDIES

In a collision zone, knowledge of the structures is necessary to establish the relationships between deformation structures, physical properties, and fluid circulations. Toward this end, every recovered structural feature was recorded and described on a form, which is a slightly modified copy of the one devised during Leg 131 (Shipboard Scientific Party, 1991) (Fig. 9).

Description and Measurements of the Structures

The terminology for macroscopic features proposed on Leg 131 was adopted and is indicated at the foot of the description form (Fig. 9). Natural structures were often difficult to distinguish from those caused by coring disturbance. Planar structures with polished surfaces and/or linear grooves were regarded as tectonic rather than drilling-induced. In zones of brecciation, features were attributed to drilling disturbance if their tectonic origin was in doubt. The recommendations of Lundberg and Moore (1986, p. 42 and 43) were followed.

Structures were first oriented relative to some "core" reference coordinates. This arbitrary reference frame was related, when possible, to true north and true vertical. Structures were measured on the face of the archive half of the split core, unless structures were significantly better preserved in the working half. The location of a structure was recorded in centimeters from the top of the section, according to ODP convention. Where a structure extended over an interval, the locations of the top and bottom of its range were recorded.

The dip of structures exposed in the split cores was recorded according to the convention illustrated in Figure 10. The plane normal to the axis of the borehole is referred to as the apparent horizontal plane. On this plane a 360° net is used with a pseudo-north (000) at the bottom line of the archive half core. Thus the face of the split core (the core face) is the plane 090/90 (strike azimuth, dip) and the plane at right angles to the core face is the plane 000/90 (strike azimuth, dip). The apparent dip on the core face, either dipping toward the east or toward the west (looking at the face of the archive half of the core with its top upward), was measured (α; example given in Fig. 10: 35°E). A second apparent dip was measured in one of two planes, depending on exposure. Usually, we measured the dip in the plane 000/90 at right angles to the core face with the apparent dip direction in this plane being toward north or south (β; example given in Fig. 10: 45°S). Sometimes we measured the dip angle on plane 000/00 where the azimuth of the line according to the core reference frame is recorded, containing directly the striking azimuth of the plane (γ; example given in Fig. 10: 55° on the plane 055/00). Dips recorded at this stage assumed that the long axis of the core is vertical; that is, deviations of the hole from vertical are ignored.

The great circle of cylindrical best fit of the two apparent dips (regarded as lines) was calculated using a Mac PC Stereonet Program (R. W. Allmendinger, Version 4.1-11). The measurements on the core face or on plane 000/90 were taken substituting N, E, S, and W with their azimuths, that is, 0°, 90°, 180°, and 270°, respectively.

The orientation of this "best-fit great circle" provided the working azimuth and dip of the observed structure within the core reference frame. The orientations of linear structures were recorded as "working trends." These were measured in the direction of plunge and referred to the core reference frame in the same way as planar surfaces. Sometimes slickensides on a fault plane were measured using the pitch (related to the vertical line of dip) on this working plane.

The sense of fault displacement was recorded and referred to as normal, reverse, or strike-slip with sinistral or dextral movements. The apparent magnitude of displacement was measured on the core face and/or on the top of broken pieces. Offset was normally measured parallel to the fault, as straight-line separation between displaced planar markers.

Real Orientation of the Structures

At this stage the structures were oriented on the core reference frame but not with respect to geographical coordinates. Real orientation depends on the availability of multishot, paleomagnetic, FMS, or BHTV data. On Leg 134, onboard correction of the data to true coordinates relied heavily on paleomagnetic and multishot information.

The multishot technique allows piston cores to be oriented and hence the arbitrary core reference frame to be positioned. However, this information is only available for the relatively shallow depths reached by the advanced piston coring system. The multishot technique provides an angle indicating the direction of a double line on the core liner with respect to magnetic north. Structural orientations are corrected by rotating the measurements by 180° + angle given by multishot + local magnetic declination (12° in the studied area) because the multishot measurement is 180° from the 000 line of the archive half of the core.

ODP Core Description: Structural Geology — Leg 134 Site_____ Hole_____ Form completed by_____

Core/ Section	Identifier*	cm from top		Dip on core-face (α)	Dip on plane 000/90 (β)	Dip on plane 000/00 (γ)	Working azimuth and dip of plane	Dip of slicken-side [pitch]	Working trend and plunge of linear	Fault sense** [N,R,S, or D]	Displace-ment [cm]	Thickness [cm]	Spacing [cm]	Paleomag. [decl./incl.]	Orient. method	Comments and Sketches
		top	bott.	[E or W]	[N or S]	[xxx/00]										

*) Possible *identifiers* include: (planar structures) bedding, scaly fabric, faults, joints, shear/deformation bands, veins, pseudo-veins, fissility, fold axial surfaces; (linear structures) slickensides, fibers, fold axes. The terms may be modified by the terms: discrete, diffuse, planar/parallel, conjugate, trapezoidal, anastomosing, bifurcating, or sinuous. **) N = normal, R = reverse, S = sinistral, D = dextral

Figure 9. An example of the description form (modified from Shipboard Scientific Party, 1991) used for recording structural features.

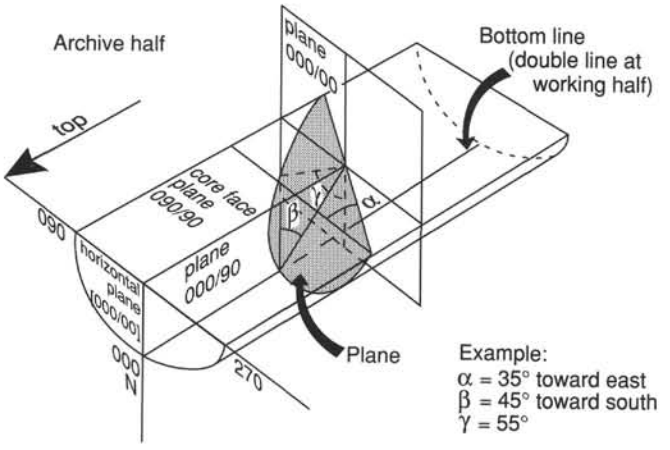

Figure 10. Sketch of the archive half of the core showing the conventions used for measuring azimuths and dips of structural features.

Paleomagnetic measurements were obtained on the core using a pass-through cryogenic magnetometer and on discrete samples taken from the core. Where these measurements provide the declination and inclination of the natural remanent magnetism, the NRM can be used for orienting the structures. This method is useful on unoriented cores obtained using the rotary and extended piston coring systems, which often disrupt the core by breaking it into several pieces that rotate independently of each other within the core liner. These drilling-induced rotations can sometimes be estimated and removed on the basis of magnetic declination of the archive half measured using the pass-through cryogenic magnetometer. The method assumes that each segment with constant value is a homogeneous drilling biscuit. Paleomagnetic convention employs a "pseudo-north" or 000 direction in the working half of the core at 180° with respect to our reference frame based on the archive half. Orientation of the structural features using magnetic data thus requires a rotation of 180° minus the magnetic declination. In some cases, a component of viscous remanent magnetization (VRM) parallel to the present-day magnetic field can be used to orient cores.

Corrections of the drift from vertical of the hole can be made only from multishot data. Deviations from vertical were consistently less than 5° and hence could be neglected.

Orientations that were possible aboard ship are presented in the site descriptions. Some of the interpretations will be refined after further work, such as correlation with FMS (Cisowski et al., 1990) and BHTV, which can only be done after processing of these data.

Presentation of Structural Data

Structural data observed in the cores are reported in structural logs, which are included in the "Structural Studies" section of each site chapter. Figure 11 shows the legend for the symbols used in these tables. The dip of bedding is indicated in a separate column. We added a question mark to the points representing a bedding plane when we could measure only the apparent dip on the core face or when the identification as a bedding plane was not certain. We subdivided the structural features into three categories: faults, scaly fabrics, or other features (e.g., shear zone, microfold, and cataclasite). Repetition of symbols at a single horizon is used to indicate qualitatively the amount of deformation. The inclination of the symbols representing faults or shear zones is taken from the values measured in the cores. Additional information is given in the "Comments" column.

Figure 11. Legend for the structural logs included in the "Structural Studies" sections of master columns in the site chapters.

Subdivision of Structural vs. Tectonic Units

When an obvious tectonic boundary (such as a thrust plane or inverted stratigraphic section) divides the recovered interval, we used the term "tectonic unit" to refer to the subdivisions. If we observed no distinct tectonic boundaries, we distinguished between degrees of deformation within lithostratigraphic units by using the term "structural unit." We identified tectonic units at Sites 827 through 830 and structural units at Sites 832 and 833. We described no structures at Site 831.

PHYSICAL PROPERTIES

Shipboard determinations of physical properties are the basis for geotechnical stratigraphy studies and provide a very important link between the geophysical seismic survey data, electrical downhole logging results, and the visual geologic record obtained by coring. It is the combination of these three data sets that provides a clearer, integrated view of the seafloor around the borehole. The goal of the physical properties program during Leg 134 was to quantify, in as much detail as possible, the changes that different sediment and rock units have undergone as a result of their involvement in the tectonic processes associated with the collision of the d'Entrecasteaux Zone (DEZ) with the central New Hebrides Island Arc.

The physical properties (PP) routinely measured aboard the *JOIDES Resolution* are index properties, compressional (*P*-wave) or shear (*S*-wave) sonic velocity, undrained vane shear strength, thermal conductivity, and formation factor. They are defined as follows:

1. Index properties: gravimetric determinations of wet, dry, and grain density, porosity, and water content.
2. Compressional or shear-wave sonic velocity: the speed of sound in sediments or rock, measured in both the vertical and horizontal directions.
3. Vane shear strength: a relative indicator of the strength of undrained sediment by measuring its resistance to loads.
4. Thermal conductivity: the ability of sediment or rocks to transport heat.
5. Formation factor: a measurement of the ratio of the electrical resistivity of sediments to the electrical resistivity of seawater.

Thorough discussions of physical properties determination are presented by Boyce (1973, 1976), who showed that physical properties are influenced by drilling and sampling disturbance, as well as by the testing procedures used in the laboratory. For example, the water content of a particular sample may be increased by the drilling fluid (seawater) that typically surrounds a disturbed core for many hours prior to removal of the sample from the core for testing. The testing methods employed during Leg 134 are described in the order defined above. Electrical resistivity measurements were not performed on Leg 134 because the instruments had been shipped to a shore-based laboratory for calibration.

As Leg 134 was only the third ODP cruise to attempt drilling through a décollement, in general our physical properties procedures replicated as closely as possible those of the two earlier cruises that penetrated décollements, Leg 110 (Barbados Ridge) and Leg 131 (Nankai Trough). Complete and detailed reviews of the physical properties methods associated with accretionary prisms at convergent margins are contained in those volumes (Mascle et al., 1988; Shipboard Scientific Party, 1991).

Nondestructive measurements (bulk density, *P*-wave velocity, thermal conductivity) were performed on whole cores. Destructive measurements (index properties, sonic velocity, undrained vane shear strength) were conducted on individual samples taken from the working half of split cores. Samples representative of the entire core were taken with regular frequency in sections of least disturbance. Sample selection and spacing depended on the rate of core recovery, the type of measurement (see below), as well as the thickness and homogeneity of the recovered sequences.

Index Properties

Methods

Index properties are initially measured using the GRAPE, which measures bulk density on whole, undisturbed APC or XCB cores. The pycnometer and electronic balance are then used for every APC, XCB, and RCB core to measure weights and volumes of three or four individual samples per core to determine bulk density, porosity, water content, and grain density for samples when they are wet and after they have been dried in an oven. The GRAPE makes nondestructive, continuous measurements of wet-bulk density on whole cores by comparing the attenuation of gamma rays through the cores with attenuation through an aluminum standard (Boyce, 1976). After the 9.5-m (length of full recovery) cores are cut into 1.5-m sections and equilibrated to laboratory temperature, the individual sections are placed horizontally on the multisensor track (MST) and moved on a conveyor belt through the GRAPE, *P*-wave, and magnetic susceptibility sensors. The attenuation of the gamma rays passing through the liner and core was counted every 2 cm and bulk density was calculated from the attenuation values. GRAPE data were then filtered to remove values that resulted from gas, gaps, or endcap effects before averaging over 0.2-m intervals. The GRAPE was calibrated with an aluminum standard once every 24 hr. The normal GRAPE was not used to measure biscuited material in RCB cores; however, wet-bulk density on some lithified cores was determined using the special 2-min GRAPE technique as described by Boyce (1976). All bulk density data are reported in units of Mg/m^3, which is numerically equivalent to g/cm^3.

Destructive index properties determinations on discrete samples were calculated from careful measurements of wet and dry weights and wet and dry volumes on 5–15 cm^3 of sediment and rock according to procedures referenced in American Society of Testing and Materials (ASTM, 1989) and promulgated by the physical properties group of the Shipboard Measurements Panel (SMP; 30 September 1990). Index properties samples for analysis of wet- and dry-bulk density, water content, grain density, and porosity were taken immediately adjacent (in the same 10-cm interval) to measurements of sonic velocity and undrained vane shear-strength measurements. The samples (1 per core in low recovery intervals; up to 4 or 5 in full recovery cores) were placed in small aluminum beakers and weighed, with a precision of 0.02 g, using two calibrated Scientech 202 electronic balances. The sample's mass was counterbalanced by a known mass such that usually differentials of less than 2 g were measured. Samples were oven dried at 110° ± 5°C for 24 hr (ASTM, 1989). Wet and dry volumes were measured using a Quantochrome Helium Penta-Pycnometer. Weight and volume measurements were repeated until two values were within the prescribed precision of ±0.02 g and ±0.02 cm^3. Index properties were then entered into the ODP database and calculated by computer program. The sample beaker weights and volumes were checked during the transit to the first site (827), and corrected values were entered into the updated physical properties database. Dry samples were randomly selected for powdering and weight and volume measurements were repeated as a check for accuracy. Salinity-corrected physical properties were computed for all samples assuming a pore-water salinity of 35‰. The equations used by the ODP database to calculate index properties are contained in the SMP/ASTM shipboard guide (September 1990) and in Lambe and Whitman (1969), Noorany (1984), and Shipboard Scientific Party (in press). By usual convention in geotechnical engineering, the term "bulk density" refers to wet-bulk density and "porosity" refers to wet porosity, but "water content" refers to percentage of water in a sample after it has spent 24 hr drying in the oven. All physical properties measurements from Leg 134 are presented for the sake of completeness; however, the calculations of dry-bulk density, dry porosity, and wet water content are rarely used in actual practice and will not be used in our discussions unless specified.

After index properties were completed, the oven-dried samples were sent to the chemistry laboratory for powdering and calcium carbonate ($CaCO_3$) content determination using the CO_2 Coulometer method.

As a further check on shipboard grain density measurements, for the first time during Leg 134 approximately 100 g of wet material (about 30–50 cm^3) was taken and preserved for later shore-based specific gravity testing at ODP using an ASTM-approved water pycnometer. These special PP samples (10–15 total) were selected at the sampling table from representative lithologies next to the normal index properties samples, so that the results of the specific gravity tests could be directly compared.

Sonic Velocity

Methods

Sonic velocities, the compressional (*P*-) or shear (*S*-) waves traveling through sediments and rock, are hereafter referred to as V_p and V_s. Sonic velocity in the recovered core, like bulk density, was measured using two different techniques. The nondestructive technique uses the compressional or *P*-wave logger (PWL), which operates on the multisensor track along with the GRAPE, and measures V_p in whole 1.5-m sections of undisturbed APC/XCB cores. The destructive method uses the Hamilton Frame velocimeter to measure three or four discrete samples per core from the working half of the split sections for every APC, XCB, and RCB core. The PWL uses a 500-kHz compressional wave pulse at a repetition rate of 1 kHz. Both signal and receiving transducers are aligned perpendicular to the core axis. PWL measurements were set for a 2-cm interval. The PWL was calibrated with a seawater standard at least once per drill site.

Seawater was sprayed on the core liner as it moved through the MST to improve acoustic contact between the transducers and the liner. As with the GRAPE, generally only undisturbed APC cores could be measured successfully. PWL data were filtered to remove data that resulted from gas, gaps, or endcap effects. Weak returns, with signal strengths below a threshold value of 200 signal strength units, also were removed. All velocity data are reported in units of meters per second (m/s).

The Hamilton Frame velocimeter is married to a Tektronix DC 5010 counter/timer system. Leg 134 Hamilton Frame measurements were taken on discrete samples that were sufficiently competent to provide adequate signal strength. Measurements are entered into the physical properties database and sonic velocity is calculated based on the equation:

$$V = h/t, \tag{2}$$

where h = measured thickness of sample and t = traveltime through the sample.

Sample thickness (distance) is measured directly by calipers that hold the sample between the transducers on the Hamilton Frame, and wave time in microseconds is read from the Tektronix oscilloscope. Velocity samples were selected from the most intact portions of the sections with minimum disturbance, avoiding the top of the core (which is usually more disturbed), and making nearly all measurements in the same 10-cm interval and from representative lithologies. Sampling frequency increased where lithologies changed rapidly within a particular core, and samples were also taken next to the bottom of sections from which 5–25 cm of whole-rounds had been cut for interstitial water and consolidation and permeability studies. After a velocity sample of about 20 cm^3 was selected at the sampling table, 5–10 cm^3 was placed in a beaker for index properties and the rest of the sample was measured in the Hamilton Frame before being returned to the core. The subsamples for index properties were removed first because filtered seawater was used to improve the acoustic contact between the sample and the transducers. V_p was measured in both vertical (*a*-direction, parallel to the axis of the core) and horizontal (*b*- and *c*-directions, perpendicular to the axis of the core) on most cores, but velocities in either direction were not recorded when insufficient or extremely variable signals were obtained.

Samples of soft sediments were taken at the core sampling table with a small (about 20 cm^3) parallel-sided sampling scoop. A double-bladed diamond saw was used in more lithified sediments. Samples of basement rock were obtained using either a double-bladed diamond saw or a 2.5-cm-diameter rock corer. Where either of these techniques was not possible due to unconsolidated, soft, or soupy sediments and it was difficult to get a good, parallel-sided chunk of core for a measurement, velocity was measured in the Hamilton Frame horizontally through the core liner (*c*-direction only) and a correction was applied for the liner effect. In intervals of hard rock, breccia, and severely disturbed or varying lithologies, measurements were made only on competent "biscuits" or were not made at all. Every effort was made to take one measurement every other section, or at least one to three per core, depending on recovery. For measurements in which the V_p signal was noisy, the second wave, V_s, was measured instead, and these points are noted in the data. Zero traveltimes for the first and second wave through the velocity transducers were estimated by linear regressions of the traveltime vs. distance of a series of aluminum and lucite standards (Hamilton, 1971).

Shear Strength

Methods

Undrained shear strength was determined using two methods, the traditional Wykeham-Farrance spring vane-shear apparatus (SP) (Boyce 1973, 1977), and with the ODP motorized miniature vane shear (torvane device), each with a four-bladed vane having a 1:1 ratio of diameter to length of 1.28 cm. The vane was inserted into the split core section, perpendicular to the core axis, to a point where the top of the blade was covered by between 2 and 4 mm of sediment. The vane was then rotated at a rate of 89° per min until the sediment failed. The undrained shear strength was calculated from the peak torque (stress) obtained at failure. In addition to peak stress, the ODP torvane instrument graphs the output for torque vs. strain on a Hewlett-Packard XY recorder, allowing the determination of residual strength of the sediment from the post-peak values on the plotter (Mascle et al., 1988). Although it measures residual stress, the torvane requires more setup time and is not particularly quick and easy to use. As a result, during busy periods of high core recovery, the Wykeham-Farrance SP device was used much more often for vane shear-strength measurements. Testing was done only in the working half of undisturbed APC or XCB cores, and was terminated when disturbance in the split cores became significant, or when the material became too stiff and lithified for the vane to penetrate without severe cracking of the surrounding core. On RCB cores, only a few measurements of shear strength could be performed successfully, on undisturbed sections. All shear strengths are reported in units of kPa.

Thermal Conductivity

Methods

Thermal conductivity is calculated from the increase in temperature of a needle inserted into the sample and heated for a period of time. The sampled temperatures are fitted to the equation:

$$T(t) = (q/4\pi k)\, ln(t) + L(t), \quad (3)$$

where T = temperature in needle (K), q = heat input per unit length per unit time (W/ms), k = apparent thermal conductivity (W/[m · K]), t = elapsed time (s), and $L(t)$ = correction for background temperature drift, linearities from instrumental errors, and the geological inadequacies of the experiment.

Before starting thermal conductivity measurements, the whole-round core must equilibrate to room temperature for 2 to 4 hr. The probes are then inserted into four sections and the standard (every other section, if a full seven sections are recovered). Final equilibrium is determined by computer monitoring of the thermal drift in the core, which must be equal to or less than 4×10^{-2} K/min. The thermal conductivity techniques used are described by Von Herzen and Maxwell (1959) and updated by Vacquier (1985).

Soft-Sediment "Full-Space" Thermal Conductivity

Needle probes containing a heater wire and a calibrated thermistor were inserted into the sediment through small holes drilled into the liners after the cores had equilibrated to laboratory temperature (21°–24°C) and before the sections were split. The probes were carefully positioned where visual examination or MST data indicated a sample of uniform properties. Data were acquired using a Thermcon-85 unit interfaced to an IBM PC-compatible microcomputer. This system allows up to five probes to be connected and operated simultaneously. To monitor probe behavior, one probe was inserted into a standard rubber or other reference material.

Once the core was in equilibrium, the probes were heated and the temperatures were recorded during a time interval of up to 6 min, with apparent thermal conductivity calculated every 20 s. All full-space measurements were corrected for a linear offset between measured and true thermal conductivities, determined from a series of tests with standards of known conductivities. When the sediments became too stiff to allow easy insertion of the probes, holes were drilled into the core material prior to careful insertion of the probes.

Lithified-Sediment and Hard-Rock "Half-Space" Thermal Conductivity

Half-space measurements were made on selected consolidated and hard-rock samples after the cores had been split, with a needle probe sandwiched between the flat surface of a test sample and that of an epoxy block which has a relatively low conductivity. All half-space measurements were conducted in a seawater bath to keep the samples saturated, improve the thermal contact between the needle and the sample, and reduce thermal drift during the tests.

The samples were finely sandpapered to smooth the contact area and conducting compound was used to improve the thermal contact. The data collection and reduction procedures for half-space tests are identical to those for full-space tests, and the procedures have been constantly updated during recent legs (Shipboard Scientific Party, 1989) and incorporated in the shipboard thermal conductivity manual. By tests using standards of known conductivities, correction factors for each of three needles in the half-space bath were accurately updated during Leg 133 (Shipboard Scientific Party, in press) and these data were used during Leg 134. These equilibrium-drift corrections are applied by computer program over an interval of up to 6 min after probe insertion. The program accounts for the imperfect nature of the experiment (i.e., epoxy is not a perfect insulator), there is never an ideal thermal contact, the thermal compound may act as a heat sink, the heat source is not positioned exactly at the boundary between the sample and epoxy.

Data are reported in units of W/(m · K) and have an estimated error of 5%–10%. All data were corrected for *in-situ* pressure and temperature, assuming a hydrostatic pressure gradient and a temperature gradient of 110 mK/m. The pressure correction was +1% for each 1800 m. The temperature correction was +1% for each +20 K change in temperature between the laboratory and *in-situ* conditions (Ratcliffe, 1960).

REFERENCES

Adams, C. G., 1984. Neogene larger foraminifera, evolutionary and geological events in the context of datum planes. *In* Ikebe, N., and Tsuchi, R. (Eds.), *Pacific Neogene Datum Planes: Contributions to Biostratigraphy and Chronology:* Tokyo (Univ. of Tokyo Press), 47–67.

Akimoto, K., 1990. Distribution of Recent benthic foraminiferal faunas in the Pacific off Southwest Japan and around Hachijojima Island. *Sci. Rep. Tohoku Univ., Ser. 2,* 60:139–223.

American Society of Testing and Materials, 1989. *Annual Book of ASTM Standards for Soil and Rock; Building Stones:* Geotextiles (Vol. 04.08): Philadelphia (ASTM), 168–862.

Archie, G. E., 1942. The electrical resistivity log as an aid in determining some reservoir characteristics. *J. Pet. Tech.,* 5:1–8.

Backman, J., Duncan, R. A., et al., 1988. *Proc. ODP, Init. Repts.,* 115: College Station, TX (Ocean Drilling Program).

Barnes, R. O., 1988. ODP *in situ* fluid sampling and measurement: a new wireline tool. *In* Mascle, A., Moore, J. C., et al., *Proc. ODP, Init. Repts.,* 110: College Station, TX (Ocean Drilling Program): 55–63.

Berggren, W. A., Kent, D. V., and Flynn, J. J., 1985a. Jurassic to Paleogene: Part 2. Paleogene geochronology and chronostratigraphy. *In* Snelling, N. J. (Ed.), *The Chronology of the Geological Record.* Geol. Soc. London Mem., 10:141–195.

Berggren, W. A., Kent, D. V., Flynn, J. J., and Van Couvering, J. A., 1985b. Cenozoic geochronology. *Geol. Soc. Am. Bull.,* 96:1407–1418.

Berggren, W. A., Kent, D. V., and Van Couvering, J. A., 1985c. The Neogene: Part 2. Neogene geochronology and chronostratigraphy. *In* Snelling, N. J. (Ed.), *The Chronology of the Geological Record.* Geol. Soc. London Mem., 10:211–260.

Blow, W. H., 1969. Late middle Eocene to Recent planktonic foraminiferal biostratigraphy. *In* Brönniman, P., and Renz, H. H. (Eds.), *Proc. First Int. Conf. Planktonic Microfossils,* Geneva, 1967. Leiden (E. J. Brill), 1:199–422.

_____, 1979. *The Cainozoic Globigerinida:* Leiden (E. J. Brill).

Bolli, H. M., and Saunders, J. B., 1985. Oligocene to Holocene low latitude planktonic foraminifera. *In* Bolli, H. M., Saunders, J. B., and Perch-Nielsen, K. (Eds.), *Plankton Stratigraphy:* Cambridge (Cambridge Univ. Press), 155–262.

Bolli, H. M., Saunders, J. B., and Perch-Nielsen, K. (Eds.), 1985. *Plankton Stratigraphy:* Cambridge (Cambridge Univ. Press).

Boyce, R. E., 1973. Appendix I. Physical properties–methods. *In* Edgar, N. T., Saunders, J. B., et al., *Init. Repts. DSDP,* 15: Washington (U.S. Govt. Printing Office), 1115–1128.

_____, 1976. Definitions and laboratory techniques of compressional sound velocity parameters and wet-water content, wet-bulk density, and porosity parameters by gravimetric and gamma ray attenuation techniques. *In* Schlanger, S. O., Jackson, E. D., et al., *Init. Repts. DSDP,* 33: Washington (U.S. Govt. Printing Office), 931–958.

_____, 1977. Deep Sea Drilling Project procedures for shear strength measurement of clayey sediment using modified Wykeham Farrance laboratory vane apparatus. *In* Barker, P., Dalziel, I.W.D., et al., *Init. Repts. DSDP,* 36: Washington (U.S. Govt. Printing Office), 1059–1068.

Cisowski, S. M., Jarrard, R., and Koyama, M., 1990. The utilization of formation microscanner (FMS) logs to obtain azimuthal orientation of paleomagnetic samples from western Pacific ODP cores. *Eos,* 71:865.

Dankers, P. H., and Zijderveld, J.D.A, 1981. Alternating field demagnetization and the problem of gyromagnetic remanence. *Earth Planet. Sci. Lett.,* 53:89–92.

Dewen, J. T., 1983. *Essentials of Modern Open Hole Log Interpretations:* Tulsa (Penwall).

Dunham, R., 1962. Classification of carbonate rocks according to depositional texture. *In* Ham, W. E. (Ed.), *Classification of Carbonate Rocks.* AAPG, 108–121.

Embry, A. F., and Klovan, E. J., 1971. A late Devonian reef tract on northeastern Banks Island, Northwest Territories. *Bull. Can. Pet. Geol.,* 19:730–781.

Emeis, K.-C., and Kvenvolden, K. A., 1986. Shipboard organic geochemistry on *JOIDES Resolution. ODP Tech. Note,* No. 7.

Erickson, A. J., Von Herzen, R. P., Sclater, J. G., Girdler, R. W., Marshall, B. V., and Hyndman, R. D., 1975. Geothermal measurements in deep-sea boreholes. *J. Geophys. Res.,* 80:2515–2528.

Fisher, R. V., and Schmincke, H.-U., 1984. *Pyroclastic Rocks:* New York (Springer-Verlag).

Gieskes, J. M., 1973. Interstitial water studies, Leg 15: alkalinity, pH, Mg, Ca, Si, PO_4, and NH_4. *In* Heezen, B. C., MacGregor, I. D., et al., *Init. Repts. DSDP,* 20: Washington (U.S. Govt. Printing Office), 813–829.

_____, 1974. Interstitial water studies, Leg 25. *In* Simpson, E.S.W., Schlich, R., et al., *Init. Repts. DSDP,* 25: Washington (U.S. Govt. Printing Office), 361–394.

Gieskes, J. M., Blanc, G., Vrolijk, P., Elderfield, H., and Barnes, R., 1990a. Interstitial water chemistry–major constituents. *In* Moore, J. C., Mascle, A., et al., *Proc. ODP, Sci. Results,* 110: College Station, TX (Ocean Drilling Program), 155–178.

Gieskes, J. M., and Gamo, T., in press. Chemical methods for interstitial water analysis on *JOIDES Resolution. ODP Tech. Note.*

Gieskes, J. M., Vrolijk, P., and Blanc, G., 1990b. Hydrogeochemistry of the Northern Barbados Accretionary Complex Transect: ODP Leg 110. *J. Geophys. Res.,* 95:8809–8818.

Hamilton, E. L., 1971. Prediction of *in-situ* acoustic and elastic properties of marine sediments. *Geophysics,* 36:266–284.

Hay, W. W., 1970. Calcareous nannofossils from cores recovered on DSDP Leg 4. *In* Bader, R. G., Gerard, R. D., et al., *Init. Repts. DSDP,* 4: Washington (U.S. Govt. Printing Office), 455–501.

Hertzog, R., 1979. Laboratory and field evaluation of an inelastic-neutron-scattering and capture gamma-ray spectroscopy tool. *Soc. Pet. Eng. Pap.,* No. 7430.

Hyndman, R. D., Langseth, M. G., and Von Herzen, R. P., 1987. Deep Sea Drilling Project geothermal measurements: a review. *Rev. Geophys.,* 25:1563–1582.

Jaeger, J. C., 1961. The effect of the drilling fluid on temperatures measured in boreholes. *J. Geophys. Res.,* 66:563–569.

Keller, G., 1985. Depth stratification of planktonic foraminifers in the Miocene ocean. *In* Kennett, J. P. (Ed.), *The Miocene Ocean: Paleoceanography and Biogeography.* Mem. Geol. Soc. Am., 163:177–196.

Kennett, J. P., and Srinivasan, M. S., 1983. *Neogene Planktonic Foraminifera: A Phylogenetic Atlas:* Stroudsburg, PA (Hutchinson Ross).

Lambe, T. W., and Whitman, R. V., 1979. *Soil Mechanics* (SI ed.): New York (Wiley).

Lundberg, N., and Moore, J. C., 1986. Macroscopic structural features in Deep Sea Drilling Project cores from forearc regions. *In* Moore, J. C. (Ed.), *Structural Fabrics Preserved in Deep Sea Drilling Project Cores From Forearcs:* Mem. Geol. Soc. Am., 166:13–44.

Manheim, F. T., and Sayles, F. L., 1974. Composition and origin of interstitial waters of marine sediments based on deep sea drill cores. *In* Goldberg, E. D. (Ed.), *The Sea* (Vol. 5): New York (Wiley), 527–568.

Martini, E., 1971. Standard Tertiary and Quaternary calcareous nannoplankton zonation. *In* Farinacci, A. (Ed.), *Proc. 2nd Planktonic Conf. Roma:* Rome (Ed. Technosci.), 2:739–785.

Mascle, A., Moore, J. C., Taylor, E., and Shipboard Scientific Party, 1988. ODP Leg 110 at the northern Barbados Ridge: introduction and explanatory notes. *In* Mascle, A., Moore, J. C., et al., *Proc. ODP, Init. Repts.,* 110: College Station, TX (Ocean Drilling Program), 5–26.

Matthews, D. J., 1939. *Tables of Velocity of Sound in Pore Water and in Seawater:* London (Admiralty, Hydrogr. Dept.).

Mazzullo, J. M., Meyer, A., and Kidd, R., 1987. New sediment classification scheme for the Ocean Drilling Program. *In* Mazzullo, J. M., and Graham, A. G. (Eds.), *Handbook for Shipboard Sedimentologists.* ODP Tech. Note, 8:45–67.

McKee, E. D., and Weir, G. W., 1953. Terminology for stratification and cross-stratification in sedimentary rocks. *Geol. Soc. Am. Bull.,* 64:381–390.

Munsell Soil Color Charts, 1971. Baltimore, MD (Kollmonger Corp.).

Noorany, I., 1984. Phase relations in marine soils. *J. Geotech. Eng.,* 110:539–543.

Norrish, K., and Hutton, J. T., 1969. An accurate x-ray spectrographic method for the analysis of a wide range of geological samples. *Geochim. Cosmochim. Acta,* 33:431–453.

Okada, H., and Bukry, D., 1980. Supplementary modification and introduction of code numbers to the low-latitude coccolith biostratigraphic zonation (Bukry, 1973; 1975). *Mar. Micropaleontol.,* 5:321–325.

Pozzi, J. P., Martin, J. P., Pocachard, J., Feinberg, H., and Galdeano, A., 1988. In situ magnetostratigraphy: interpretation of magnetic logging in sediments. *Earth Planet. Sci. Lett.,* 88:357–373.

Ratcliffe, E. H., 1960. The thermal conductivities of ocean sediments, *J. Geophys. Res.,* 65:1535–1541.

Reynolds, R. C., 1967. Estimations of mass absorption coefficients by Compton scattering: improvements and extensions of the method. *Am. Mineral.,* 48:1133–1143.

Roperch, P., and Taylor, G. K., 1987. The importance of gyromagnetic remanence in alternating field demagnetization: some new data and experiments on GRM and RRM. *Geophys. J. R. Astron. Soc.,* 87:949–965.

Sanfilippo, A., Westberg-Smith, M. J., and Riedel, W. R., 1985. Cenozoic radiolaria. *In* Bolli, H. M., Saunders, J. B., and Perch-Nielsen, K. (Eds.), *Plankton Stratigraphy:* Cambridge (Cambridge Univ. Press), 631–712.

Sayles, F. L., Manheim, F. T., and Chan, K. M., 1973. Interstitial water studies on small core samples, Leg 4. *In* Bader, R. G., Gerard, R. D., et al., *Init. Repts. DSDP,* 4: Washington (U.S. Govt. Printing Office), 401–414.

Schlumberger, 1989. *Log Interpretation Principles/Applications:* Houston (Schlumberger Educational Services).

Serra, O., 1984. *Fundamentals of Well Log Interpretation: The Acquisition of Logging Data:* Amsterdam (Elsevier).

_____, 1989. *Formation Microscanner Image Interpretation:* Houston (Schlumberger Educational Services).

Shepard, F. P., 1954. Nomenclature based on sand-silt-clay ratios. *J. Sediment. Petrol.,* 24:151–158.

Shipboard Measurements Panel, 1990. Recommended methods for the discrete measurement of index properties on the *JOIDES Resolution:* water content, bulk density, and grain density. College Station, TX (Ocean Drilling Program).

Shipboard Scientific Party, 1988. Explanatory notes. *In* Backman, J., Duncan, R. A., et al., *Proc. ODP, Init. Repts.,* 115: College Station, TX (Ocean Drilling Program), 17–42.

_____, 1989. Introduction and explanatory notes. *In* Robinson, P. T., Von Herzen, R., et al., *Proc. ODP, Init. Repts.,* 118: College Station, TX (Ocean Drilling Program), 3–24.

_____, 1991. Explanatory notes. *In* Taira, A., Hill, I., Firth, J., et al., *Proc. ODP, Init. Repts.,* 131: College Station, TX (Ocean Drilling Program).

_____, in press. Introduction and explanatory notes. *In* Davies, P., McKenzie, J., Palmer Julson, A., et al., *Proc. ODP, Init. Repts.,* 133: College Station, TX (Ocean Drilling Program).

Timur, A., and Toksoz, M. N., 1985. Fundamentals of well log interpretation. *Annu. Rev. Earth Planet. Sci.,* 13:315–344.

Vacquier, V., 1985. The measurement of thermal conductivity of solids with a transient linear heat source on the plane surface of a poorly conducting body. *Earth Planet. Sci. Lett.,* 74:275–279.

Von Herzen, R. P., and Maxwell, A. E., 1959. The measurement of thermal conductivity of deep-sea sediments by a needle probe method. *J. Geophys. Res.,* 65:1557–1563.

Wentworth, C. K., 1922. A scale of grade and class terms for clastic sediments. *J. Geol.,* 30:377–392.

Ms 134A-106